5-1-2014

A Continuum Mechanics Approach to Modeling and Simulating Engineering Materials Undergoing Phase Transformation using the Evolving Micro-Structural Model of Inelasticity

Adetokunbo Adelana Adedoyin

A continuum mechanics approach to modeling and simulating engineering materials undergoing phase transformation using the Evolving Micro-Structural Model of Inelasticity

By

Adetokunbo Adelana Adedoyin

A Dissertation
Submitted to the Faculty of
Mississippi State University
in Partial Fulfillment of the Requirements
for the Degree of Doctor of Philosophy
in Computational Engineering
in the Department of Computational Engineering

Mississippi State, Mississippi

May 2014

A continuum mechanics approach to modeling and simulating engineering materials undergoing phase transformation using the Evolving Micro-Structural Model of Inelasticity

By

Adetokunbo Adelana Adedoyin

Approved:

Douglas J. Bammann (Major Professor)	Youssef Hammi (Dissertation Co-advisor)

Thomas E. Lacy
(Committee Member)

Seongjai Kim
(Committee Member)

Edward A. Luke
(Committee Member)

Roger L. King
(Graduate Coordinator)

Achille Messac
Dean
Bagley College of Engineering

Name: Adetokunbo Adelana Adedoyin

Date of Degree: May 16, 2014

Institution: Mississippi State University

Major Field: Computational Engineering

Major Professor: Dr. Douglas J. Bammann

Title of Study: A continuum mechanics approach to modeling and simulating engineering materials undergoing phase transformation using the Evolving Micro-Structural Model of Inelasticity

Pages of Study: 82

Candidate for Degree of Doctor of Philosophy

Heat treatment for the purpose of material strengthening is accompanied by residual stresses and distortion. During these processing steps, steel alloys experience a phase change that in turn modify their overall mechanical response. To properly account for the cumulative composite behavior, the mechanical response, transformation kinetics and subsequent interaction of each phase have to be properly accounted for. Of interest to material designers and fabricators is modeling and simulating the evolutionary process a part undergoes for the sake of capturing the observable residual stress states and geometric distortion accumulated after processing.

In an attempt to capture the aforementioned physical phenomena, this investigation is premised upon a consistent thermodynamic framework. Following this, the single phase Evolving Microstructural Model of Inelasticity state variable model is extended to accommodate the occurrence of multiphases, affirming that the interaction between coexisting

phases is through an interfacial stress. Since the efficacy of a multiphase model is dependent on its ability to capture the behavior of constituents phases and their subsequent interaction, we introduce a physically based self-consistent strain partitioning algorithm.

With synthesis of the aforementioned ideas, the additional transformation induced plasticity is numerically accounted for by modifying each phase's flowrule to accommodate an interfacial stress. In addition, for simulating the cohabitation of two phases, the mechanical multiphase model equations is coupled with a previously developed non-diffusional phase transformation kinetics model. A qualitative assessment of the material response based on a Taylor, Sachs and self-consistent polycrystalline approximation is carried out. Further analysis of the multiphase model and its interaction with transformation kinetics is evaluated.

Key words: Plasticity, Phase Transformation, Multiphase, Rate Kinetics, Polycrystalline Approximation

DEDICATION

To all involved in the advancement of knowledge in continuum mechanics and its application to metal inelasticity.

ACKNOWLEDGEMENTS

This work was supported by the Center for Advanced Vehicular Systems at Mississippi State University. I am grateful to Dr. Douglas J. Bammann for directing this research. Most importantly, I appreciate his relentless effort towards mentoring and providing a surplus of keen insight into problem solving; irrespective of the difficulty level. I have also learnt from Dr. Bammann that every problem has an anchor and as a Scientist and Engineer it is your responsibility to search for it. He has also thought me to press-on in attempting to solve a problem and refining the solution as i move along in acquiring knowledge.

I choose my committee members with the criterion being courses that were known to require some rigor on both the part of the student and Instructor. Most importantly, I was in search for mentors that were excellent in their respective fields. I appreciate the effort of Dr. Thomas E. Lacy Jr. for his patient in teaching me Continuum Mechanics, Dr. Seongjai Kim for his shrewdness in communicating a numerical view on Partial Differential Equations and Dr. Edward A. Luke for his theoretical rigor in teaching parallel computing. I pray that their effort towards mentoring students not go in vain. I am also grateful for their comments on this dissertation.

Special thanks to Dr. Esteban Marin, Dr. Youssef Hammi, Dr. Kofi Enakoutsa and Dr. Sule Dogan for their relentless support both educational and emotional during this effort.

Lastly, I am grateful to God for my parents, Mr. Simeon Shina and Mrs. Henrietta Kikelomo Adedoyin, and my immediate siblings for their continuous support in my past, present and future endeavor.

TABLE OF CONTENTS

LIST OF TABLES

LIST OF FIGURES

MODEL NOMENCLATURE

$TRIP$ Transformation Induced Plasticity

$EMMI$ Evolving Micro-Structural Model of Inelasticity

SSD Statistically stored dislocations

GND Geometrically necessary dislocations

σ, $\boldsymbol{\sigma}$ Scalar and 2^{nd} rank Cauchy stress tensor

$\boldsymbol{\alpha}$ 2^{nd} rank tensorial kinematic hardening variable

κ, $\boldsymbol{\kappa}$ Scalar and 2^{nd} rank tensorial isotropic hardening variable

$\mathbf{S}$ 2^{nd} rank tensorial deviatoric stress

$\mathbf{p}$ 2^{nd} rank tensorial pressure

π, $\boldsymbol{\pi}$ Scalar and 2^{nd} rank tensorial Interfacial stress

$\mathbf{l}$ 2^{nd} rank tensorial velocity gradient

$\mathbf{w}$ 2^{nd} rank tensorial asymmetrical velocity gradient

$\mathbf{d}$ 2^{nd} rank tensorial symmetrical velocity gradient

$\mathbf{I}$ 2^{nd} rank tensorial identity

$\boldsymbol{\epsilon}_l$ 2^{nd} rank tensorial lattice strain tensor

ϵ_{ss}, $\boldsymbol{\epsilon}_{ss}$ Scalar and 2^{nd} rank tensorial statistically stored dislocations strain tensor

$\boldsymbol{\epsilon}_\beta$ 2^{nd} rank tensorial geometrically necessary dislocations strain tensor

ϵ_π, $\boldsymbol{\epsilon}_\pi$ Scalar and 2^{nd} rank tensorial interface strain

ψ Helmholtz free energy

ϕ Volume fraction of martensite

CHAPTER 1

INTRODUCTION

1.1 Literature Review

Practitioners have been largely successful in developing heat treatment protocols based on experience. A significant amount of steel parts are successfully heat treated to meet product requirements. These heat treatment protocols can successfully reproduce the required hardness profiles, carbon profiles or microstructure of the part. Modeling, however, still plays a vital role in dimensional control. It attempts to predict dimensional changes that occur during heat treatment. Computational models can be used to determine how the local thermal histories affect phase transformation. Dimensional changes can stem from a combination of either thermal expansion or contraction, long term creep operating at high temperatures, carborization, transformation plasticity, and transformation strains. For reasons such as computational efficiency, modeling the heat treatment process using a continuum mechanics framework is still an attractive option. It requires research into a broad range of topics.

According to Truesdell [97, 98] research efforts in continuum mechanics are focused mainly on three major areas. One area spans the development of constitutive equations that represent material behavior derived based on experimentation, microscopic modeling or experience. Another area encompasses employing a numerical analysis approach to

deal with a selected constitutive formulation. Finally, other challenges include performing a mathematical analysis involving the governing equations. Here the main focus is in developing a multiphase inelasticity model that incorporates phase transformation kinetics. Therefore, most of the research effort here is concentrated in the first two aforementioned subject areas. In general, the research effort in multiphase inelasticity includes a discussion on several subtopics namely thermodynamics, kinematics, polycrystalline partitioning and transformation kinetics models for coexisting phases.

The pioneering working of Truesdell and Noll [97, 98] on developing, composing and documenting the nonlinear-field theories of mechanics has fostered the extensive application of continuum mathematics to modeling of engineering materials exhibiting non-linear behavior. Subsequent works of Coleman and Noll [24,25] on finding the restrictions placed on the constitutive formulation designed to account for the dissipative effects expressed through heat conduction and subsequent deformation helped propel the application of thermodynamics to continuum mechanics. Based on the approach taken by [24, 25], Coleman and Gurtin [23] derived the thermodynamics restrictions necessary when applying Internal State Variables (ISVs) to modeling materials that exhibit nonlinear behavior using a continuum mechanics framework

The works of Eshelby [29,30] on determination of the elastic field in and around an ellipsoidal inclusion encouraged the development of view point of a framework for handling materials with discontinuous properties. Further works of Ericksen [28], Ball [9] encouraged the development of an approach to mathematically model the existence of multiphases in an elastic solid. A number of researchers [8, 101] through experimentation, theoretical

derivation and calculation have established the fact that martensite develops 24 possible variants in the presence of an austenite phase with each variant showing a distinct lattice orientation.

It has been well documented [22] that phase changes can be viewed as a forced rearrangement or reorganization of a lattice to accommodate an external driving function. From this point of view, it is conceivable that there will be an associated straining due to the appearance of a product phase or phases during heat treatment or quenching procedures. The onset these product phases is preceded by additional plastic flow usually referred to as Transformation Induced Plasticity (TRIP) known to be explained by two mechanisms namely the Greenwood-Johnson [41] or accommodation process and the Magee [76] mechanism or orientation process. Following Leblond et al. [65], TRIP is the additional plasticity due to the evolution of the constituent phase fractions of a transformation prone material. Previous works on multiphase modeling using continuum theory have explicitly included an additional strain to account for the TRIP [3]. This additional strain is simply a numerical quantity introduced to account for the straining observed during a phase change.

A similar approach was taken in the early development of modeling techniques or formulation to account for creep phenomena [84]. It became common practice to introduce a creep strain in addition to the plastic strain, resulting in an expression for the inelastic strain. Since creep is simply the rate or time dependent deformation observed in crystalline material at elevated temperatures and constant stress boundary conditions, it is often the same dislocation-based mechanism associated with plastic flow in tension tests constant velocity boundary condition. To remedy this apparent inconsistency, several rate depen-

dent plasticity models have been introduced. These models were capable of predicting both rate dependent creep and classical plasticity without the introduction of a yield surface and were commonly referred to as Unified Creep Plasticity (UCP) model [20, 58, 81, 100].

In the past, several researchers have demonstrated the possibility of extending a continuum mechanics based formulation with ISVs to modeling of co-existing phases. Tanaka and Nagaki [92] devised an approach for modeling engineering materials experiencing phase transition. They introduce two ISVs, one that kept track of crystallographic structure evolution and the other that measures the extent of phase transition. To model the interaction or effects of parent and product phases they introduce a TRIP strain quantity to account for the additional plasticity experienced during phase transformation. In an attempt to capture the plasticity induced as a result of phase transition, Leblond et al. [61,64] used the Hill-Mandel [44,77] homogenization process to decompose the macroscopic plastic strain into two contributing portions. They decompose the macroscopic plastic strain into a contribution from classical plasticity and the other from transformation plasticity without a priori assumption of a new microscopic plastic strain.

In a later work, Leblond et al. [62,63] experimented with previously proposed relationships between the macroscopic TRIP stain-rate quantity and the stress deviator [37, 60]. Subsequently, neglecting the Magee mechanism, they pursued a numerical investigation of the TRIP component with a consideration of both perfectly-plastic (negligible hardening) and strain hardening effects. It is noteworthy to mention that based on experimental observations several other authors [1, 36, 41, 82] had derived constitutive relationships between

macroscopic TRIP stain or strain rate and stress analogous to the form of the flow law for classical plasticity.

Bammann et al. [10,11,15,16] developed an ISV framework that enabled capturing the temperature and stain rate dependent behavior observable in single phase materials, resulting in the Bammann-Chelsea-Johnson (BCJ) plasticity model. The kinematic hardening phenomena was captured using a tensorial state variable with a cast in a hardening minus recovery format following Frederick and Armstrong [34]. Similarly to the kinematic hardening evolution, isotropic hardening evolution though a scalar state variable, was cast in a similar hardening minus recovery format. In a subsequent work, Bammann et al. [12] extend the BCJ single phase framework to capture the occurrence of coexisting phases in an engineering material. The effort was directed toward capturing the residual stress and distortion observable in the event of a welding, heat treatment or quenching procedures performed on low alloy steels.

Several finite deformation kinematic frameworks have been proposed to enable capturing the phase transformation phenomena observed in crystalline materials. The more common mathematical framework used to formulate the kinematics of finite deformation for a single phase is based on a multiplicative decomposition of the deformation gradient (F) into an elastic and plastic component. Following Khan [52], the deformation gradient can be decomposed into:

$$\mathbf{F} = \mathbf{F}_e \mathbf{F}_p \tag{1.1}$$

where $\mathbf{F}_e$ and $\mathbf{F}_p$ is the elastic and plastic part. In a similar manner, this approach has been extended to a multiphase framework. Bock and Holzapfel [19], Kroner [59], and Lee and

Liu [66] extended the small strain phase transition framework work earlier developed by Leblond et al. [62, 63] to a large strain framework. They accounted for the additional plasticity relating to the orientation process (Magee Effect) [76]. The evolution law accounting for the TRIP strains was chosen to be of a visco-plastic nature.

More recently, Hallberg et al. [43] using a large-strain plasticity framework proposed a phase transition model to describe martensitic formation in austenitic steels. For the thermodynamic formulation, their choice of state variable included the elastic strain, a hardening variable, temperature and the phase volume fraction of martensite. Using a Crystal plasticity framework, Tjahjanto et al. [96] modeled the Transformation plasticity phenomenon. Based on a finite strain framework they decompose the deformation gradient into:

$$\mathbf{F} = \mathbf{F}_e \mathbf{F}_p \mathbf{F}_{tr} \tag{1.2}$$

where $\mathbf{F}_e$, $\mathbf{F}_p$ and $\mathbf{F}_{tr}$ is the elastic, plastic and transformation deformation gradient component. A similar model development approach as described above had been taken by numerous authors [18, 67–69, 89–91] where the fundamental difference in the model approach may lie in either the TRIP strain formulation and or incorporation, the kinematic assumption, the scale of interest, the choice of internal state variable or the phase evolution kinetics model used.

In simulating multiphase, a decision has to be made on how the strain rate or velocity gradient is partitioned into each phase. Several techniques have been developed in the past to satisfy either equilibrium, compatibility or a combination of both. Assuming infinitesimal strains and imposing a Taylor [93–95] approximation (compatibility), the strain rate

tensor decomposes uniform in the polycrystalline material. The magnitude of the far field strain rate will be imposed into all present phases uniformly. A Sachs [88] approximation, however, requires proportional loading in all phases implying that the imposed boundary condition is proportionally distributed into each phase. As documented by Kocks et al. [54], Budiansky and Wu [21] and a host of others as have attempted to develop a polycrystalline model that combines the benefits of both the Sachs and the Taylor model. This hybrid approach is commonly referred to as a self-consistent approximation, it satisfies neither compatibility nor equilibrium but combines the physical features of both models. According to Knocks et al. [54], "self-consistent polycrystal models aim at deducing the overall response of the aggregate from the known properties of the constituent grains and an assumption concerning the interaction of each grain with its environment."

In the past, several researchers have developed phase transformation kinetics models that can be incorporated into a continuum framework. These models of transformation kinetics are classified into two groups namely diffusional (Avarami [5, 6]), and non-diffusional (Koistinen-Marberger [55]) models . Non-diffusional models are used to capture phase evolution from austenite to martensite while diffusional models help capture austenite to ferrite, pearlite or banite transformations. A previous work worthy of note is that of Kolmogorov [57] on metal crystallization. Similar to the arguments posed by Avarami [5], but in this case for crystallization, Kolmogorov [57] derives a generalized form for probabilistically determining the number of crystal centers combined to form a crystal bulk within a crystal volume. Today several researchers are given credit for the development of the models for capturing the kinetics of diffusional phase transfor-

mation. These models are commonly referred to as JMAK after Johnson and Mehl [50], Avarami [5–7] and Kolmogorov [57]. In recent years, Lusk et al. [72–74] developed a model for both diffusional and non-diffusional phase transformation. They premised the development of their model with balance principles and incorporate some of the underlying physics of phase transformation. A two-phase system is considered here. These phases are qualitatively associated with martensite and austenite where the transformation is a non-diffusion type. The focus is on low to mild carbon steels.

The rapid development in computer architecture coupled with industrial demand for high resolution and low cost computer simulations has led to the continuous development of numerical tools for simulating heat treatment. Ferguson et al. [32, 33], developed DANTE R a heat treatment subroutine that interfaces with ABAQUS [78]. Using DANTE R , several numerical studies have been conducted in an attempt to better understand the physics of heat treatment and quenching. The development of DANTE R has also fostered collaborative efforts [70, 71, 99, 102]. Other tools such as HEARTS [46, 47], SYSWELD [48] and TRAST [83] have also been developed. The aforementioned tools work as either stand-alone packages or in a plug-in type fashion into well know table-top multi-physics packages like COMSOL [26], ABAQUS [78], SolidWorks [79] and so on.

CHAPTER 2

APPLICATION OF PHYSICALLY BASED PLASTICITY MODEL TO MATERIALS UNDERGOING PHASE TRANSFORMATION

2.1 Abstract

Heat treatment for the purpose of material strengthening is accompanied by residual stresses and distortion. During these processing steps, steel alloys experience a phase change that in turn modifies their mechanical response. To properly account for the cumulative composite behavior, the properties of each phase and subsequent interactions have to be properly accounted for.

In an attempt to capture the aforementioned physical phenomena, we extend the single phase continuum based Evolving Microstructural Model of Inelasticity (EMMI) framework to capture the occurrence of coexisting phases. Since the efficacy of a multiphase model is dependent on its ability to capture the behavior of constituents phases and their subsequent interaction, we introduce a physically based self-consistent partitioning algorithm. A quantitative assessment of the material response based on a Taylor, Sachs and self-consistent polycrystalline approximation is carried out.

2.2 Introduction

It is common practice in the material fabrication industry to attempt to improve upon the service life of a part. Practitioners have been largely successful in developing heat treatment recipes based on trial and error. A significant amount of steel parts are successfully being heat treated to meet product requirements such as hardness profiles, carbon profiles and microstructure. Modeling, however, still plays a vital role in dimensional control. It attempts to predict dimensional changes that occur during heat treatment. It's purpose being computationally determine how the local thermal histories affect phase transformation. These dimensional changes stems from a combination of either thermal expansion or contraction, long term creep operating at high temperatures, carborization, transformation plasticity and transformation strains.

Several attempts have been made to capture the effects of this underlying physical phenomena, however, often with limited success. Modeling phase transformation with the observation that the lattice difference between coexisting phases indicates a discontinuity in the yield strength does not capture the volume change or any resulting plasticity [27,38]. An attempt to capture the volume change by solely introducing large changes in thermal expansion physically neglects any additional plasticity resulting from phase transformation and in addition may be purely phenomenological, completely missing the underlying physics [38,39,89,90]. Models that attempt to numerically elucidate the physical phenomena by explicitly accounting for the associated volume change many times do not correctly capture the sign and magnitude of the apparent residual stresses [38, 40, 86].

It has been well documented [22] that phase change can be viewed as a forced rearrangement or reorganization of a lattice to accommodate an external driving function. From this point of view, it is conceivable that there will be an associated straining due to the appearance of a product phase or phases during a heat treatment or quenching procedure. Previous works on multi-phase modeling via continuum theory have explicitly included an additional strain to account for the transformation induced plasticity (TRIP) [3] as described by [41, 75]. This additional strain is simply a numerical quantity introduced to account for the straining observed during a phase-change or a new phase-resurface. A similar approach was taken in the early development of modeling techniques or formulation for the creep phenomena [84]. It became common practice to introduce a creep strain quantity that was added to the plastic strain, resulting in an expression for the inelastic strain. Since creep is simply the rate or time dependent deformation observed in materials at elevated temperatures and constant stress boundary conditions, it is often the same dislocation based mechanism associated with plastic flow in tension tests at constant velocity boundary condition. To remedy this apparent inconsistency, several rate dependent plasticity models have been introduced. These models were capable of predicting both rate dependent creep and classical plasticity without the introduction of a yield surface and were commonly referred to as Unified Creep Plasticity (UCP) models [20, 58, 81, 100].

Rather than introducing a phenomenological TRIP strain, a more physically meaningful approach is to attempt to capture the effects of a naturally imposed interfacial stress between discontinuous lattice structure types [49]. With the aforementioned point of view on capturing creep, TRIP can be implicitly captured by observing that the product phase

only requires accounting for the interfacial stress resulting from the incompatibility between juxtaposed phases. Understanding that the inclusion of a new material in a matrix is mathematically analogous specifying an interfacial stress with which both materials can interact is key. In addition, since it is well understood [28] that phase transformation is a shear induced process, there is an additional stipulation on the direction of the imposed interfacial stresses.

Motivated by the need to develop a better understanding of heat treatment and quenching of metal alloys, the continuum based EMMI [80] framework has being extended to capture the occurrence of more than a single phase coexisting in an engineering material. While a similar approach was taken in previous implementation [12–14, 16, 87], however, with the Bammann-Chelsea-Johnson (BCJ) plasticity model, the purpose of this paper is to extend the aforementioned ideas and give them a stronger physical and thermodynamic foundation. Here, we use a two-phase system and qualitatively associate these phases with austenite and martensite. Available to us is experimental data of 5120 steel over a limited strain rate and temperature regime were. The goal of this is to eventually extend this work to all five phases in an attempt to modify and extend the approach taken by previously by Bammann et al. [12–14, 16]. Of interest here are materials that undergo phase transformation that consequentially modifies the material macroscopic response. The belief is that a proper continuum mechanics based formulation with internal state variables is sufficient to capture the underlying physical phenomena and in turn recover the appropriate magnitude and direction of the resulting residual stresses and distortion.The following mathematical operations in direct notation are used in the remainder of this paper. They are defined

as follows. Given a second rank tensorial quantity $\mathbf{A}$, it follows that $\|\mathbf{A}\| = (\mathbf{A} : \mathbf{A})^{1/2}$, $Tr(\mathbf{A}) = (\mathbf{A} : \mathbf{I})^{1/2}$ and $\acute{\mathbf{A}} = \mathbf{A} - \frac{1}{3} Tr(\mathbf{A})\, \mathbf{I}$.

2.3 Methodology

2.3.1 Multiphase EMMI Constitutive Equations

In order to extend the EMMI model to capture the effects of materials undergoing phase transformation, while the dislocation based internal state variable (ISV) model is developed for finite strain, the assumption that each continuum point is occupied by both a parent and a product phase had to be made. Using a volume fraction weighted rule of mixtures the Cauchy stress in the current configuration is determined to be of the form:

$$\boldsymbol{\sigma} = \sum_{i=1}^{n} \phi^{(i)} \boldsymbol{\sigma}^{(i)} \tag{2.1}$$

where $\acute{\boldsymbol{\sigma}}^{(i)}$ represents the Cauchy stress in each phase and the superscript indicate the i^{th} phase. The subsequent volume fraction is given by: $\phi^{(i)}$:

$$\phi^{(i)} = (1 - \sum_{j \neq i}^{n} \phi^{(j)}). \tag{2.2}$$

The phases considered here are austenite and martensite and therefore the Cauchy stress simply reduces to:

$$\boldsymbol{\sigma} = \phi^{(1)} \boldsymbol{\sigma}^{(1)} + \phi^{(2)} \boldsymbol{\sigma}^{(2)} \tag{2.3}$$

with $\phi^{(1)}$ and $\phi^{(2)}$ representing the austenite and martensite phases. Therefore the volume fraction for martensite and austenite phases is simply represented by ϕ and $1 - \phi$, respec-

tively. From the assumption of linear elasticity, and for a homogeneous isotropic material the hypoelastic relation for each phase is given by:

$$\mathring{\boldsymbol{\sigma}}^{(i)} = \frac{\boldsymbol{\sigma}^{(i)}}{\mu^{(i)}}(\frac{d\mu^{(i)}}{d\theta})^{(i)}\dot{\theta}^{(i)} + \lambda^{(i)}tr(\mathbf{d}_e^{(i)})\mathbf{I} + 2\mu^{(i)}\mathbf{d}_e^{(i)} \tag{2.4}$$

where $\lambda^{(i)}$ and $\mu^{(i)}$ represent the temperature dependent first and second $Lam\acute{e}$ parameters for each phase. $\theta^{(i)}$ is the temperature in each phase, $\mathbf{d}_e^{(i)}$ is the elastic part of the symmetrical portion of the velocity gradient in each phase and $\mathbf{I}$ is the three dimensional identity tensor. The convective derivative of the Cauchy stress is of the form:

$$\mathring{\boldsymbol{\sigma}}^{(i)} = \dot{\boldsymbol{\sigma}}^{(i)} - \mathbf{w}_e^{(i)}\boldsymbol{\sigma}^{(i)} + \boldsymbol{\sigma}^{(i)}\mathbf{w}_e^{(i)} \tag{2.5}$$

where $\mathbf{w}_e^{(i)}$ is the elastic part of the asymmetrical portion of the velocity gradient in each phase. The elastic asymmetrical portion of the velocity gradient for each phase is:

$$\mathbf{w}_e^{(i)} = \mathbf{w}^{(i)} - \mathbf{w}_p^{(i)} - \mathbf{w}_\theta^{(i)} \tag{2.6}$$

where the total, plastic and thermal parts are $\mathbf{w}^{(i)}$, $\mathbf{w}_p^{(i)}$ and $\mathbf{w}_\theta^{(i)}$, respectively. Similarly the symmetrical portion of the velocity gradient is:

$$\mathbf{d}_e^{(i)} = \mathbf{d}^{(i)} - \mathbf{d}_p^{(i)} - \mathbf{d}_\theta^{(i)} \tag{2.7}$$

where the total, plastic and thermal parts are $\mathbf{d}^{(i)}$, $\mathbf{d}_p^{(i)}$ and $\mathbf{d}_\theta^{(i)}$, respectively. The partitioning of the total velocity gradient based on it's constituent spin and stretch is will be dependent on the polycrystal model chosen. Numerically integrating the hypoelastic relation Eqn. (2.4) requires decomposing the stress rate into it constituent deviatoric and hydrostatic portions. The deviatoric stress rate is of the form:

$$\dot{\mathbf{s}}^{(i)} = \frac{\mathbf{s}^{(i)}}{\mu^{(i)}}(\frac{d\mu^{(i)}}{d\theta})\dot{\theta}^{(i)} + 2\mu^{(i)}\acute{\mathbf{d}}_e^{(i)} - \mathbf{w}_e^{(i)}\mathbf{s}^{(i)} + \mathbf{s}^{(i)}\mathbf{w}_e^{(i)} \tag{2.8}$$

while the pressure rate tensor is given by:

$$\dot{\mathbf{p}}^{(i)} = \frac{\mathbf{p}^{(i)}}{K^{(i)}}(\frac{dK^{(i)}}{d\theta})\dot{\theta}^{(i)} + K^{(i)}Tr\left(\mathbf{d}_e^{(i)}\right)\mathbf{I} - \mathbf{w}_e^{(i)}\mathbf{p}^{(i)} + \mathbf{p}^{(i)}\mathbf{w}_e^{(i)} \tag{2.9}$$

The form of the temperature dependent portion of each material property was chosen following the approach taken by Marin et al. [80]. The shear modulus for each phase $\mu^{(i)}$ is of the form:

$$\mu^{(i)} = \mu_0^{(i)}\hat{\mu}\left(\theta\right)^{(i)} \tag{2.10}$$

where $\mu_0^{(i)}$ is the shear modulus at room temperature. Following Frost and Ashby [35], $\hat{\mu}\left(\theta\right)^{(i)}$ is chosen to be the form of the temperature dependent portion of the shear modulus at all temperatures:

$$\hat{\mu}\left(\theta\right)^{(i)} = 1 + c_{\theta\mu}^{(i)}\frac{\theta^{(i)} - \theta_0^{(i)}}{\theta_m^{(i)}} \tag{2.11}$$

where the temperature factor is:

$$c_{\theta\mu}^{(i)} = \frac{\theta_m^{(i)}}{\mu_0^{(i)}}\frac{d\mu^{(i)}}{d\theta} < 0 \tag{2.12}$$

$\theta^{(i)}$ represents the temperature of the material, $\theta_0^{(i)}$ represents the reference temperature and θ_m the melt temperature for each phase. Similarly the bulk modulus $K^{(i)}$ for each phase is chosen to be of the form:

$$K^{(i)} = K_0^{(i)}\hat{K}\left(\theta\right)^{(i)} \tag{2.13}$$

where $K_0^{(i)}$ is the bulk modulus at room temperature, $\hat{K}\left(\theta\right)^{(i)}$ is chosen to be the form of the temperature dependent portion of the bulk modulus at all temperatures. The form of the temperature dependence of the bulk modulus is assumed following Frost and Ashby [35]:

$$\hat{K}\left(\theta\right)^{(i)} = 1 + c_{\theta K}^{(i)}\frac{\theta^{(i)} - \theta_0^{(i)}}{\theta_m^{(i)}} \tag{2.14}$$

where the temperature factor is:

$$c_{\theta K}^{(i)} = \frac{\theta_m^{(i)}}{K_0^{(i)}} \frac{dK^{(i)}}{d\theta} < 0 \tag{2.15}$$

$\theta^{(i)}$ represents the temperature of the material, $\theta_0^{(i)}$ represents the reference temperature and $\theta_m^{(i)}$ the melt temperature for each phase. The evolution law for the 2^{nd} rank tensorial kinematic hardening state variable ($\boldsymbol{\alpha}$) cast in a hardening and recovery format following Frederick and Armstrong [34] is given by:

$$\begin{aligned} \mathring{\boldsymbol{\alpha}}^{(i)} &= \frac{\boldsymbol{\alpha}^{(i)}}{\mu^{(i)}} (\frac{d\mu}{d\theta})^{(i)} \dot{\theta}^{(i)} + 2\mu^{(i)} h^{(i)} C_a^{(i)} \sqrt{\frac{3}{2}} \mathbf{d}_p^{(i)} \\ &- \frac{r_d^{(i)}}{2\mu^{(i)} C_a^{(i)}} \sqrt{\frac{2}{3}} \dot{\epsilon}_p^{(i)} \quad \boldsymbol{\alpha}^{(i)} \quad \boldsymbol{\alpha}^{(i)} \end{aligned} \tag{2.16}$$

where the hardening and dynamic recovery parameters for each phase is represented by $h^{(i)} = \hat{h}(\theta, C)$ and $r_d^{(i)} = \hat{r}_d^{(i)}(\theta)$. Here θ and C imply a dependence on temperature and carbon content, respectively. The hat serves to distinguish the value of the hardening variable from it functional dependence. $\dot{\epsilon}_p^{(i)}$ is the scalar plastic strain rate while $\mathbf{d}_p^{(i)}$ is the plastic part of the 2^{nd} rank tensorial velocity gradient. The convective derivative of the kinematic state variable is of the form:

$$\mathring{\boldsymbol{\alpha}}^{(i)} = \dot{\boldsymbol{\alpha}}^{(i)} - \mathbf{w}_e^{(i)} \boldsymbol{\alpha}^{(i)} + \boldsymbol{\alpha}^{(i)} \mathbf{w}_e^{(i)} \tag{2.17}$$

The rate form of the scalar isotropic hardening state variable ($\kappa^{(i)}$) in each phase determined by Kock and Mecking [53], Estrin and Mecking [31] and Nes [85] cast in a hardening and recovery format is given by:

$$\begin{aligned} \dot{\kappa}^{(i)} &= \frac{\kappa^{(i)}}{\mu^{(i)}} (\frac{d\mu}{d\theta})^{(i)} \dot{\theta}^{(i)} + 2\mu^{(i)} H^{(i)} C_k^{(i)} \dot{\epsilon}_p^{(i)} \\ &- R_d^{(i)} \kappa^{(i)} \dot{\epsilon}_p^{(i)} - R_s^{(i)} \kappa^{(i)} \sinh \left[\frac{Q_s^{(i)} \kappa^{(i)}}{2\mu^{(i)} C_k^{(i)}} \right] \end{aligned} \tag{2.18}$$

and similarly the $H^{(i)} = \hat{H}^{(i)}(\theta, C)$ is the hardening parameter in each phase. $R_s^{(i)} = \hat{R}_s^{(i)}(\theta)$ and $R_d^{(i)} = \hat{R}_d^{(i)}(\theta)$ are the static and dynamic recovery parameter in each phase. $C_k^{(i)}$ is the isotropic parameters in each phase. The constitutive equation governing plastic flow is presumed to be of the form:

$$\mathbf{d}_p^{(i)} = \sqrt{\frac{3}{2}}\dot{\epsilon}_p^{(i)}\acute{\mathbf{N}}^{(i)} \tag{2.19}$$

where $\acute{\mathbf{N}}$ is the unit normal deviatoric $2^{(i)}$ rank tensorial quantity in the direction of the net effective deviatoric stress for each phase. The plastic flow rate ($\dot{\epsilon}_p^{(i)}$) for each phase is given by:

$$\dot{\epsilon}_p^{(i)} = f^{(i)} \sinh \left[\frac{\sqrt{\frac{3}{2}} \acute{\boldsymbol{\xi}}^{(i)} \pm \pi^{(i)}}{\kappa^{(i)} + Y^{(i)}(\theta)} - 1 \right]^{n^{(i)}} \tag{2.20}$$

where $f^{(i)}$ the transition material parameter for each phase. $n^{(i)}$ is the plastic exponent in each phase. $Y^{(i)}$ and $\hat{Y}^{(i)}(\theta)$ are the temperature dependent yield strength and the form of the temperature dependence of the yield strength in each phase. $\acute{\boldsymbol{\xi}}^{(i)}$ is the net effective stress in each phase. The direction of plastic flow in each phase is given by:

$$\acute{\mathbf{N}}^{(i)} = \frac{\acute{\boldsymbol{\xi}}^{(i)}}{\acute{\boldsymbol{\xi}}^{(i)}}. \tag{2.21}$$

The norm of the net effective stress is given by:

$$\acute{\boldsymbol{\xi}}^{(i)} = \acute{\boldsymbol{\sigma}}^{(i)} - \frac{2}{3}\acute{\boldsymbol{\alpha}}^{(i)} \tag{2.22}$$

The temperature dependent yield strength in each phase given by:

$$Y^{(i)} = 2\mu_0^{(i)} c_8^{(i)} \hat{Y}\,(\theta)^{(i)} \tag{2.23}$$

where $c_8^{(i)}$ is the yield parameter in each phase fitted to experimental data. The form of the temperature dependence of the yield strength is assumed to be:

$$\hat{Y}\left(\theta\right)^{(i)} = \frac{m_1^{(i)}}{1 + m_2^{(i)} \exp\left(\frac{-m_3^{(i)}}{\theta}\right)} \frac{1}{2}\left[1 + \tanh\left(m_4^{(i)}(m_5^{(i)} - \theta)\right)\right]. \tag{2.24}$$

The thermal part of the symmetric portion of the velocity gradient in each phase is given by:

$$\mathbf{d}_\theta^{(i)} = \dot{\epsilon}_\theta^{(i)}\mathbf{I} \tag{2.25}$$

where $\dot{\epsilon}_\theta^{(i)}$ represent the thermal strain rate as a result of thermal expansion or contraction in each phase. The thermal strain rate is given by:

$$\dot{\epsilon}_\theta^{(i)} = f_\beta(\theta)^{(i)}\dot{\theta} \tag{2.26}$$

where $f_\beta(\theta)^{(i)}$ is the thermal expansion coefficient in each phase given by:

$$f_\beta(\theta)^{(i)} = \frac{\beta(\theta)^{(i)} - \beta_0^{(i)} b_\theta^{(i)}(\theta - \theta_0)}{1 - \beta(\theta)^{(i)}(\theta - \theta_0)} \tag{2.27}$$

where $\beta_0^{(i)}$ is a thermal parameter. The form of the temperature dependence of the thermal expansion coefficient $\beta(\theta)^{(i)}$ in each phase given by:

$$\beta(\theta)^{(i)} = \beta_0^{(i)}(1 - b_\theta^{(i)}(\theta - \theta_0)) \tag{2.28}$$

The interfacial stress is determined to act in a manner where prior to the appearance of a second phase, the parent phase must experience a zero interfacial stress. Implying that the interfacial stress evolution must vanish at a parent phase volume fraction of unity. Following this idea, we make the assumption that interfacial stress rate is of the form:

$$\dot{\pi} = C_\pi \frac{\Delta V}{V}\left[\dot{\phi} - 2\phi\dot{\phi}\right] \tag{2.29}$$

where C_π is the interfacial stress parameter. $\frac{\Delta V}{V}$ is the lattice change due to carbon addition.

The formulation of the interfacial stress evolution implemented here stipulates that communication between each phase is through an interaction stress π^i where each phase imposes its presence on all others and vise versa. This representative form of communication between each phase stipulates that the interaction between each phase is strictly through and resulting from each phases volume fraction, volume fraction rate and volume change. In the absence of an evolving volume fraction the interfacial stress ceases to evolve leading to a constant inter-phase interaction stress. The transformation from austenite into martensite occurs via a shearing process. Here, we treat the interfacial stress in the same manner as the scalar hardening internal state variable κ, as acting in a non-directional manner. In a future work, we will utilize an orientation tensor to introduce the directionality of the interfacial (π) stress into the model, naturally incorporating the shearing aspects of the transformation process.

Noting the linear relationship between the interfacial stress rate $\dot{\pi}$ and the phase volume fraction rate $\dot{\phi}$ at constant volume, the interfacial stress rate equation Eqn. (2.29) can be integrated to yield the interfacial stress experienced by either phase corresponding to a specific phase volume fraction. For a two phase model, at the onset of the appearance of a product phase, the interfacial stress experienced by the austenite and martensite stress yields:

$$\pi = C_\pi \frac{\Delta V}{V} \left[\phi - \phi^2\right] \tag{2.30}$$

A useful check is to ensure that integrating equation Eqn. (2.29) for both phases at their respective integral limits yield the same quantity for the interfacial stress relation. That is:

$$\int_{1}^{1-\phi} \pi(\phi^{(1)}) d\phi^{(1)} \equiv \int_{\phi}^{1} \pi(\phi^{(2)}) d\phi^{(2)} \tag{2.31}$$

2.3.2 Additional Considerations: Polycrystalline Approximation

In an attempt to satisfy the requirements of a polycrystal model several techniques have been developed in the past to satisfy either equilibrium, compatibility or a combination of both. For the decomposition of the symmetric part of the velocity gradient assuming a Taylor [93–95] approximation (compatibility) requires uniform straining in a multiphase material. Following equation Eqn. (2.7) all phases experience the magnitude of the symmetric velocity gradient therefore the elastic symmetric portion of the velocity gradient in each phase is of the form:

$$\mathbf{d}_e^{(i)} = \mathbf{d} - \mathbf{d}_p^{(i)} - \mathbf{d}_\theta^{(i)}. \tag{2.32}$$

For the case where there is negligible plasticity and thermal straining, the upper bound on the stress field is proportional to the symmetric portion of the velocity gradient:

$$\boldsymbol{\sigma}^{(i)} \propto \mathbf{d} \tag{2.33}$$

A Sachs [88] approximation requires proportional straining in all phases implying that the far-field forcing function is proportional to that experienced in each phase. For a two phase model, the austenite phase experiences a stretch rate proportional to the far field strain rate:

$$\mathbf{d}^{(1)} = (1-\phi)\mathbf{d} \tag{2.34}$$

where $1-\phi$ represent the volume fraction of the austenite phase. Similarly, the martensite phase experiences a stretch rate proportional to the far field strain rate, therefore:

$$\mathbf{d}^{(2)} = (\phi)\mathbf{d} \tag{2.35}$$

For the case where $\phi = 0$ we recover a single phase model. When $\phi = 1$ a complete transformation in the material has occurred from austenite to martensite. Using a Sachs [88] argument, the coefficient of proportionality at the upper and lower bounds of the volume fraction must satisfy the constraint:

$$(1-\phi)\phi = 0 \tag{2.36}$$

mathematically enforcing a bound for the martensitic volume fraction ϕ such as:

$$0 \leq \phi \leq 1 \tag{2.37}$$

Budiansky and Wu [21] and a host of others as documented by Kocks et al. [54] have attempted to develop a polycrystalline model that combines the benefits of both the Sachs and the Taylor model. Commonly referred to as a self-consistent approximation, it satisfies neither compatibility nor equilibrium but combines the physical features of both models.

According to Knocks et al. [54], "self-consistent polycrystal models aim at deducing the overall response of the aggregate from the known properties of the constituent grains and an assumption concerning the interaction of each grain with its environment." With this in mind, we modify the requirements on the proportionality constants Eqn. (2.36) and replace the scalar volume fraction with a functional constraint:

$$(1-f(\phi))f(\phi) = 0 \tag{2.38}$$

therefore the response of a satisfactory function $f(\phi)$ must satisfy the Eqn. (2.37). Therefore we can replace Eqn. (2.34) and Eqn. (2.35) with:

$$\mathbf{d}^{(1)} = (1 - f(\phi))\,\mathbf{d} \tag{2.39}$$

and

$$\mathbf{d}^{(2)} = (f(\phi))\,\mathbf{d} \tag{2.40}$$

The efficacy of the multiphase model is dependent on the ability of each constituent part to capture the underlying physical behavior therefore implementing a physically based portioning algorithm is important. We determine that a functional form that satisfies the constraint Eqn. (2.38) is sufficient; such as those used in determining a self-consistent approximation or as applied in percolation theory. We propose:

$$f(\phi) = \frac{1}{2}\left(1 + \tanh\left[C_1\left(\phi - C_2\right)\right]\right) \tag{2.41}$$

where C_1 determines the profile of the partitioning function. Analogous to inclusion used in material strengthening, further investigation will be directed towards determining the relationship between the shape parameter C_1 and martensitic spheroidal particles or platelets and how they affect the partitioning profile. The parameter C_2 is a transition parameter that determines the volume faction at which the martensite phase starts to experience the intensity of the strain field upon yielding of the softer austenite phase.

Figure 2.1 is strain rate as appropriated to each phase based on a Sachs, Taylor and a self-consistent polycrystalline approximation at a strain rate of $\dot{\epsilon} = 1/s$. The self-consistent model the parameters C_1 = 4, 6, 11 and C_2 = 0.5. The Taylor model, represented by the horizontal line at $\dot{\epsilon} = 1/s$, shows each phase experiences the same strain rate

at all volume fractions of martensite. The Sachs model however, represented by a linear line through the origin, requires that each phase experiences a strain rate proportional to it's respective volume fractions. The self-consistent polycrystalline approximation using the constraint Eqn. (2.38) captures a more physical interaction between the mechanical properties of constituent phases.

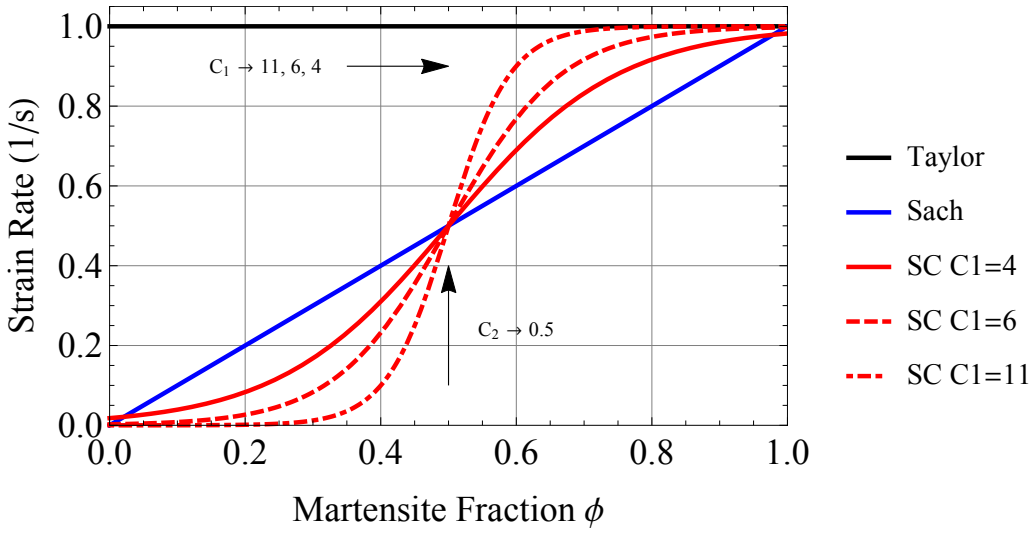

Figure 2.1

Strain rate partitioning for Sachs, Taylor and a self-consistent (SC_i) polycrystalline approximation at $\dot{\epsilon}$ = 1/s.

2.4 Results

A quantitative assessment of the multiphase EMMI model was performed with the help of a number of simplifying assumptions. We assumed isothermal conditions. For the cases implemented here the material parameters were assumed to be a fit for a fixed carbon

content, therefore $\frac{\Delta V}{V} = 1$. Uniaxial tension tests for 5120 stainless steel were performed at a range of temperatures and strain rates.

Collected data was used to determine the EMMI model parameters for respective phases. A gradient based optimization routine was used to determine EMMI Model parameters as listed on Table 2.1 following the approach taken by Marin et al. [80]. The material properties used here is that of stainless steel 304L (SS304L). Table 2.2 is a tabulation of the material properties used in this study. Figure **??** is the EMMI model response fitted to experimental data of 5120 martensite steel for uniaxial tension for martenite. Experimental data if for uniaxial tension at strain rate $\dot{\epsilon} = 0.1/s$ and temperature θ_{1-3}=296.15, 423.15, 598.15 (K). Figure **??** is the EMMI model response fitted to experimental data of 5120 martensite steel for uniaxial tension for austenite and martenite. Experimental data if for uniaxial tension at strain rate $\dot{\epsilon}_{1-3}$ = 0.01,0.1,0.01 (1/s) and temperature θ_{1-3}=1073, 1123, 1223 (K).

For an assessment of the material response based on a Taylor, Sachs and self-consistent polycrystalline approximation three combinations of volume fraction for both phases were tested. A combination of $90\%A + 10\%M$, $50\%A + 50\%M$ and $10\%A + 90\%M$ were used, where A and M stand for austenite and martensite. The resulting deviatoric stress field for all cases were determined using Eqn. (2.3). The parameter values chosen for the self-consistent approximation are $c_1 = 3.68$ and $c_2 = 0.5$.

At 10% martensite Figure 2.4, the self -consistent and Sachs models are expected to predict a similar deviatoric stress field. This is because the value of the proportionality functional in the self-consistent and Sachs are of very close. The result is physically mean-

Table 2.1

Material parameters for 5120 austenite and martensite steel.

Parameter	Symbol	Magnitude	Unit
Hardening	$H^{(1)}$	1.19E-3	-
Hardening	$H^{(2)}$	4.71E-2	-
Dynamic Recovery	$R_d^{(1)}$	1.67E-3	-
Dynamic Recovery	$R_d^{(2)}$	1.20E-1	-
Static Recovery	$R_s^{(1)}$	9.81E-57	1/s
Static Recovery	$R_s^{(2)}$	4.34E-55	1/s
	$Q_s^{(1)}$	1	-
	$Q_s^{(2)}$	1	-
	$C_\kappa^{(1)}$	1	-
	$C_\kappa^{(2)}$	1	-
Hardening	$h^{(1)}$	1.1E-1	-
Hardening	$h^{(2)}$	1.1E-1	-
Dynamic Recovery	$r_d^{(1)}$	629935	-
Dynamic Recovery	$r_d^{(2)}$	285457	-
	$C_a^{(1)}$	1	-
	$C_a^{(2)}$	1	-
Transition Constant	$f^{(1)}$	1.13E-4	1/s
Transition Constant	$f^{(2)}$	2.27E-6	1/s
Plastic Exponent	$n^{(1)}$	2.29	-
Plastic Exponent	$n^{(2)}$	15.16	-

Table 2.2

Material properties for stainless steel 304L (SS304L).

Parameter	Symbol	Magnitude	Unit
Yield	m_1	1.2854	-
Yield	m_2	2.6999	-
Yield	m_3	614.628	K
Yield	m_4	9.60774E-3	1/K
Yield	m_5	1139.68	K
Yield	c_8	5.5168E-3	-
Elastic	E	210979	MPa
Lame I	λ	121540	MPa
Bulk	k	175645	MPa
Bulk	$c_{\theta k}$	-0.36	-
Shear	μ	81157.8	MPa
Shear	$c_{\theta \mu}$	-0.85	-

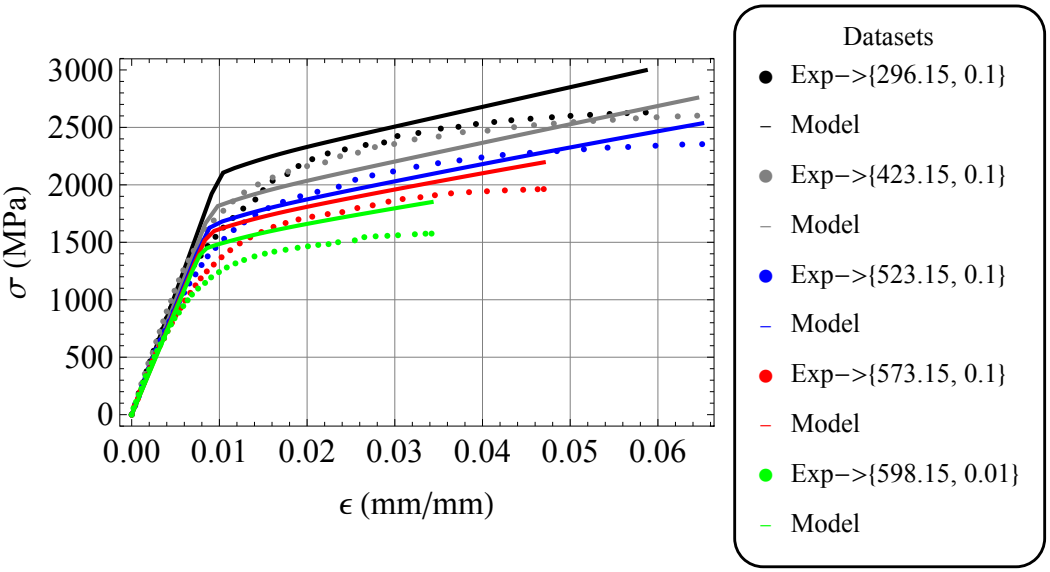

Figure 2.2

EMMI model response fitted to experimental data of 5120 martensite steel.

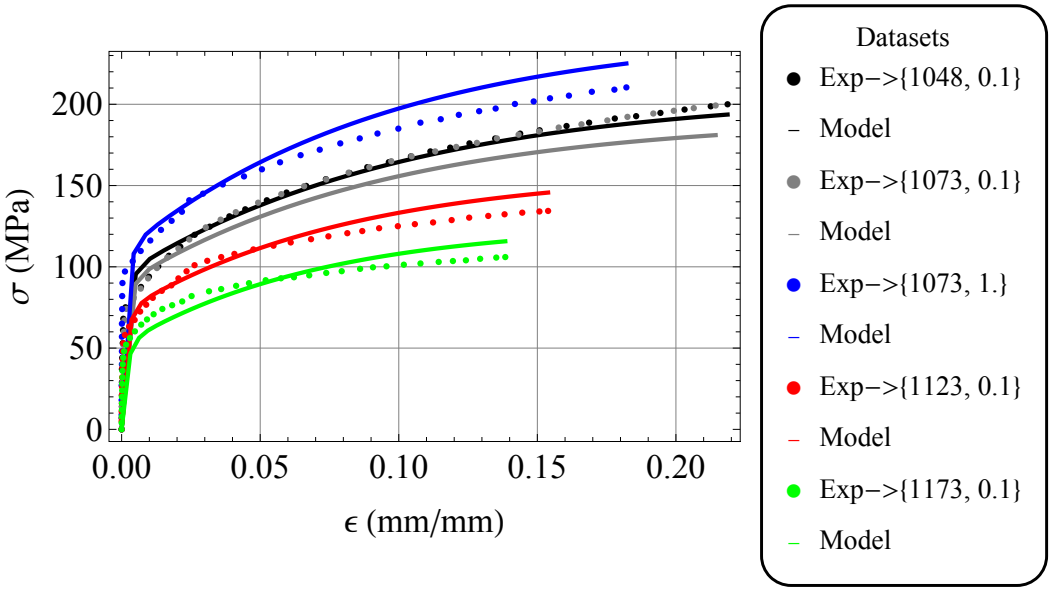

Figure 2.3

EMMI model response fitted to experimental data of 5120 austenite steel.

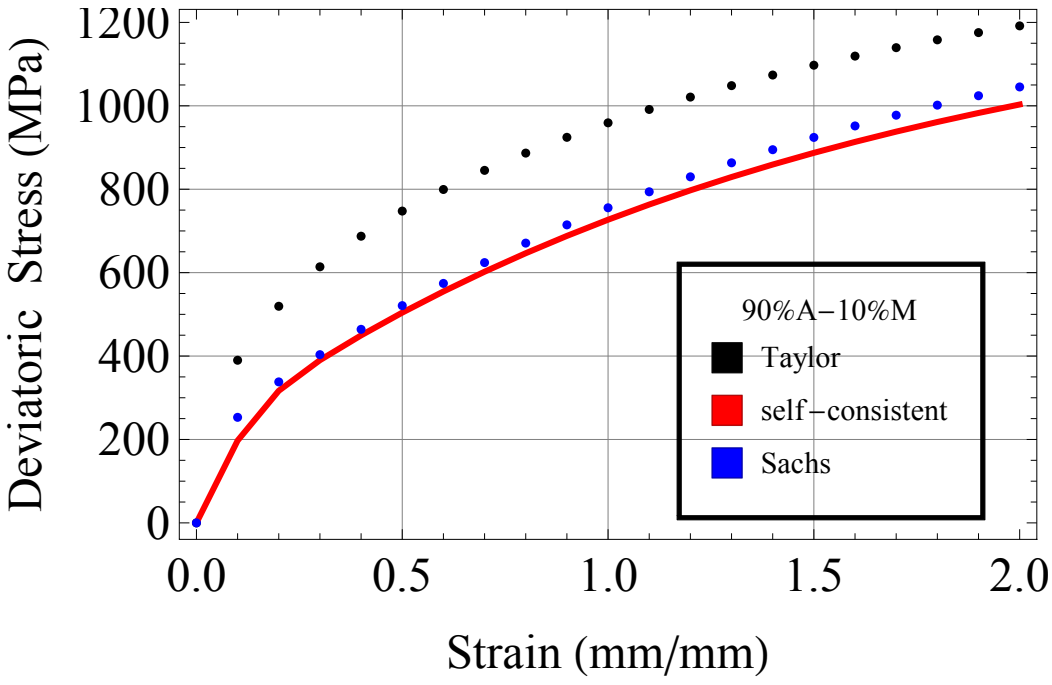

Figure 2.4

$\acute{\boldsymbol{\sigma}}_1$ for Taylor, Sachs and self-consistent approximation at $90\%A + 10\%M$.

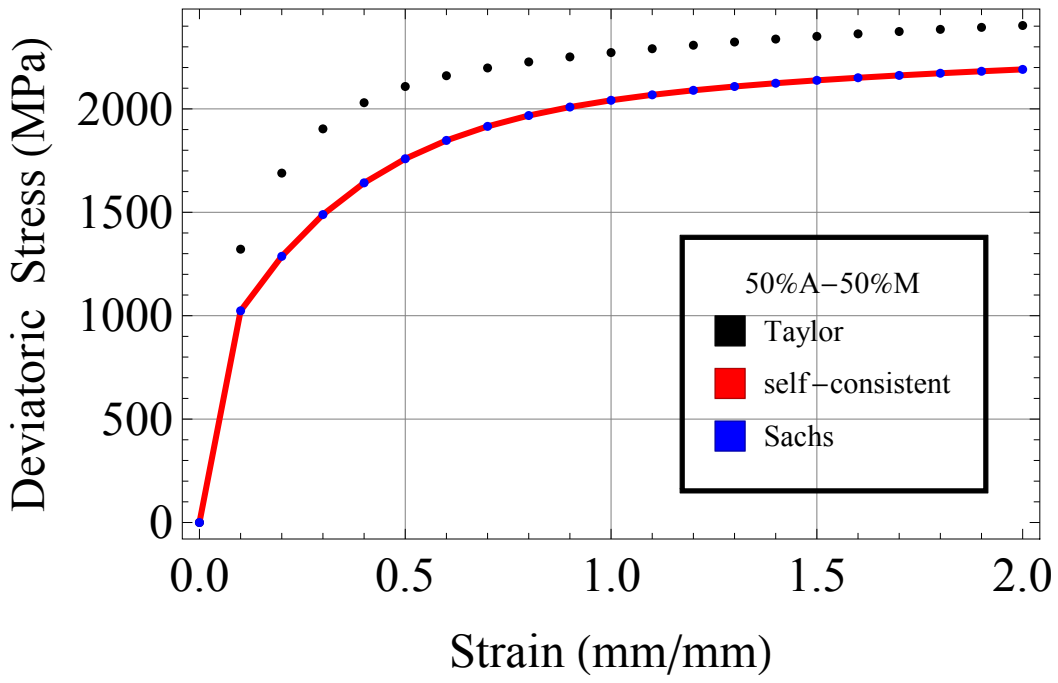

Figure 2.5

$\acute{\boldsymbol{\sigma}}_1$ for Taylor, Sachs and self-consistent approximation at $50\%A + 50\%M$.

ingful because the stress field in general should not deviate much from a predominantly austenitic field irrespective of the material properties of the martensite. The disparity in the resulting deviatoric stress field from the Taylor model when compared with the Sachs and self-consistent is because both phases experience the same straining; this is in most cases non physical.

Similarly, at 50% martensite Figure 2.5, the self-consistent and Sachs approximations are expected to predict exactly the same magnitude of deviatoric stress field. This is because the transition parameter for the self-consistent approach was chosen to match exactly exactly at $\phi = 0.5$. The difference however with the Taylor assumption in emphasized by the difference in the internal state variable material parameter.

At 90% martensite Figure 2.6, there is very little distinction between a Taylor, Sachs or self-consistent approximation. For a self-consistent and Sachs approach the dominant strain rate in carried by the martensite which is naturally imposed using a Taylor approximation.

2.5 Summary

The EMMI single phase internal state variable model was extended to accommodate the presence of product phases. We assumed a two-phase system where the mechanical response and transformation kinetics model for austenite and martensite were qualitatively associated with austenite and martensite. Available is experimental data of 5120 steel over a limited strain rate and temperature regime.

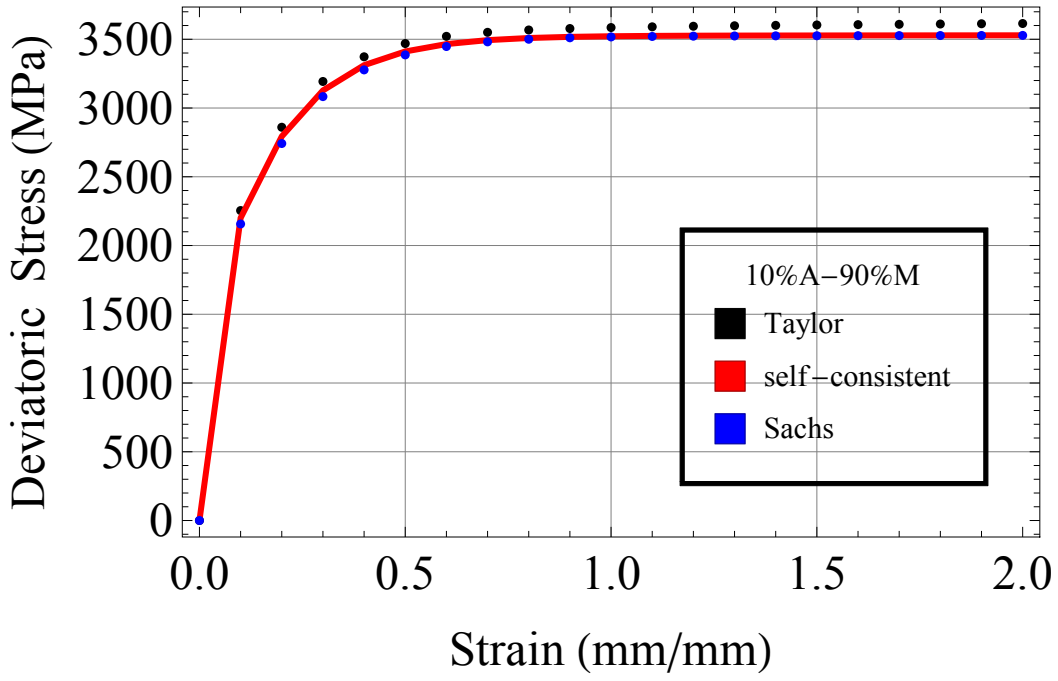

Figure 2.6

$\acute{\boldsymbol{\sigma}}_1$ for Taylor, Sachs and self-consistent approximation at $10\%A + 90\%M$.

The additional TRIP was accounted for through the introduction of a physically appropriate interfacial stress acting as a forward stress in the softer austenite, and a backward stress in the martensite. Since the efficacy of a multiphase model is dependent on its ability to capture the behavior of constituents phases and their subsequent interaction, we introduce a physically based self-consistent partitioning algorithm. A quantitative assessment of the material response and plastic flow based on the Taylor, Sachs and self-consistent approximation was carried out.

CHAPTER 3

A QUALITATIVE ASSESSMENT OF THE MULTIPHASE EMMI PLASTICITY MODEL COUPLED WITH PHASE TRANSFORMATION KINETICS

3.1 Abstract

Commonly implemented material processing routines not limited to quenching, welding or heat treatment requires exposure of a part to complex thermal and mechanical loading histories that in turn manifest as residual stress and distortion. Of interest to material designers and fabricators is modeling and simulating the evolutionary process a part undergoes for the sake of capturing this observable residual stress states and geometric distortion accumulated after processing.

In an attempt to move toward an overall consistent modeling approach, we premise this investigation with a consistent thermodynamic framework. Following this, we extend the single phase Evolving Microstructural Model of Inelasticity (EMMI) internal state variable model to multiphase affirming that the interaction between coexisting phases is through an interfacial stress. We then employ a self-consistent polycrystalline model in order to partition each individual phase's strain field ensuring a hybrid between compatibility and equilibrium. With a synthesis of the aforementioned ideas, the additional transformation plasticity (TRIP) is numerically accounted for by modifying each phase's flowrule to accommodate an interfacial stress. In addition, for simulating the cohabitation of two phases

we couple the mechanical multiphase model equations with a previously developed non-diffusional phase transformation kinetic model.

3.2 Introduction

The pioneering working of Truesdell and Noll [97, 98] on developing, composing and documenting the nonlinear-field theories of mechanics has fostered the extensive application of continuum mathematics to modeling of engineering materials exhibiting non-linear behavior. Subsequent works of Coleman and Noll [24,25] on finding the restrictions placed on the constitutive formulation designed to account for the dissipative effects expressed through heat conduction and subsequent deformation helped propel the application of thermodynamics to continuum mechanics. Based on the approach taken by [24, 25], Coleman and Gurtin [23] formulated a continuum thermodynamics framework for the application of Internal State Variables (ISVs) to modeling the nonlinear behavior of engineering materials.

The works of Eshelby [29, 30] on determination of the elastic field in and around an ellipsoidal inclusion encouraged the development of view point of a framework for handling materials with discontinuous properties. Further works of Ericksen [28], Ball [9] encouraged the development of an approach to mathematically model the existence of multiphases in an elastic solid. A number of researchers [8, 101] through experimentation, theoretical derivation and calculation have established the fact that martensite develops 24 possible variants in the presence of an austenite phase with each variant showing a distinct lattice orientation.

In the past, several researchers have demonstrated the possibility of extending a continuum mechanics based formulation with ISVs to modeling of co-existing phases. Tanaka and Nagaki [92] devised an approach for modeling engineering materials experiencing phase transition. They introduce two ISVs, one that kept track of crystallographic structure evolution and the other that measures the extent of phase transition. To model the interaction or effects of parent and product phases they introduce a TRIP strain quantity to account for the additional plasticity experienced during phase transformation. In an attempt to capture the plasticity induced as a result of phase transition, Leblond et al. [61,64] used the Hill-Mandel [44,77] homogenization process to decompose the macroscopic plastic strain into two contributing portions. They decompose the macroscopic plastic strain into a contribution from classical plasticity and the other from transformation plasticity without a priori assumption of a new microscopic plastic strain.

In an attempt to capture the plasticity induced as a result of phase transition, Leblond et al. [61, 64] via the Hill-Mandel [44, 77] homogenization process decompose the macroscopic plastic strain into two contributing portions. More notably, they decompose the macroscopic plastic strain into a contribution from classical plasticity and the other from transformation plasticity without a priori assumption of a new microscopic plastic strain. In a later work, Leblond et al. [62, 63] experimented with previously proposed relationship between the macroscopic TRIP stain-rate quantity and the stress deviator [37, 60]. Subsequently, neglecting the Magee mechanism [76], they pursued a numerical investigation of the transformation induced plasticity component with a consideration of both perfectly-plastic and strain hardening effects. It is noteworthy to mention that based on experimen-

tal observations several other authors [1, 36, 41, 82] had derived constitutive relationships between macroscopic TRIP strain or strain rate and stress analogous to the form of the flow-law for classical plasticity.

Previously, Bammann et al. [10, 11, 15, 16] developed an ISV framework that enabled capturing the temperature and strain rate dependent behavior observable in engineering materials notably the Bammann-Chelsea-Johnson (BCJ) plasticity model. The well established kinematic hardening phenomena was captured using a tensorial state variable where it's rate was cast in a hardening minus recovery format following Ashby [4].

Similarly to the format of the kinematic hardening rate state variable, isotropic hardening rate though a scalar variable, was cast in a hardening minus recovery format. In a subsequent work, Bammann et al. [12] extend the BCJ single phase framework to capture the occurrence of coexisting phase in an engineering material. The effort was directed toward capturing the residual stress and distortion observable in the event of a welding, heat treatment or quenching procedure performed on low alloy steels.

Several finite deformation kinematic frameworks have been proposed to enable capturing the phase transformation phenomena observed in crystalline materials. The more common mathematical framework used to formulate the kinematics of finite deformation for a single phase is based on a multiplicative decomposition of the deformation gradient (F) into an elastic and plastic component. Following Khan [52], the deformation gradient can be decomposed into:

$$\mathbf{F} = \mathbf{F}_e \mathbf{F}_p \tag{3.1}$$

where $\mathbf{F}_e$ and $\mathbf{F}_p$ is the elastic and plastic part. In a similar manner, this approach has been extended to a multiphase framework. Bock and Holzapfel [19], Kroner [59], and Lee and Liu [66] extended the small strain phase transition framework work earlier developed by Leblond et al. [62, 63] to a large strain framework. They accounted for the additional plasticity relating to the orientation process (Magee Effect) [76]. The evolution law accounting for the TRIP strains was chosen to be of a visco-plastic nature.

More recently, Hallberg et al. [43] using a large-strain plasticity framework proposed a phase transition model to describe martensitic formation in austenitic steels. For the thermodynamic formulation, their choice of state variable included the elastic strain, a hardening variable, temperature and the phase volume fraction of martensite. Using a Crystal plasticity framework, Tjahjanto et al. [96] modeled the Transformation plasticity phenomenon. Based on a finite strain framework they decompose the deformation gradient into:

$$\mathbf{F} = \mathbf{F}_e\mathbf{F}_p\mathbf{F}_{tr} \tag{3.2}$$

where $\mathbf{F}_e$, $\mathbf{F}_p$ and $\mathbf{F}_{tr}$ is the elastic, plastic and transformation deformation gradient component. A similar model development approach as described above had been taken by numerous authors [18, 67–69, 89–91] where the fundamental difference in the model approach may lie in either the TRIP strain formulation and or incorporation, the kinematic assumption, the scale of interest, the choice of internal state variable or the phase evolution kinetics model used.

Continuum mechanics as an approach to modeling and simulating engineering material behavior is attractive. Its mathematical framework enables scientist and engineers capture

the behavior of a material in an average manner. Effectively coupling phase kinetics models to a continuum mechanics framework requires several consideration. One of which includes homogeneity, that is, uniform without irregularities, have to be made in order to deem a material point differentiable or continuous where in a numerical sense, the imposed differentiability would allow for a discretizable subset space. It would only be reasonable to assume that each continuum point can readily accommodate evolving new phases. With this approach, phase transformation kinetics can be modeled. Similarly, conservation of energy or similar principles can be estimated as a cumulative sum of each cohabiting phase. In addition, the cumulative stress may then be deduced using a volume fraction weighted rule of mixtures.

Today several researchers are given credit for the development of the equation for modeling the kinetics of phase transformation of a diffusional or non-diffusional type. Common diffusional models are commonly referred to as JMAK after Johnson and Mehl [50], Avarami [5–7] and Kolmogorov [57]. For a non-diffusional transformation the Koistinen-Marburger [56] model (KM) or some form of it is the most widely adopted model for austenite to martensite transformation. In more recent years, Lusk et al. [72–74] have experimented with similar approaches to phase transformation kinetics where they premise the development of their model with the balance principle for both diffusional and non-diffusional types. Of consideration here are non-diffusion type models with a focus on low to mild carbon steels.

The rapid development in computer architecture coupled with industrial demand for high resolution and low cost computer simulations has led to the continuous develop-

ment of numerical tools for simulating heat treatment. Ferguson et al. [32, 33], developed DANTE R a heat treatment subroutine that interfaces with ABAQUS [78]. Using DANTE R , several numerical studies have been conducted in an attempt to better understand the physics of heat treatment and quenching. The development of DANTE R has also fostered collaborative efforts [70, 71, 99, 102]. Other tools such as HEARTS [46, 47], SYSWELD [48] and TRAST [83] have also been developed. The aforementioned tools work as either stand-alone packages or in a plug-in type fashion into well know table-top multi-physics packages like COMSOL [26], ABAQUS [78], SolidWorks [79] and so on.

Motivated by the need to develop a better understanding of heat treatment and quenching of metal alloys, the continuum based EMMI framework has being extended to capture the occurrence of more than a single phase coexisting in an engineering material. Of interest here are materials that undergo phase transformation that consequentially modifies the material mechanical response. Here in we premise this investigation with a consistent thermodynamic framework. Following this, we extend the single phase EMMI plasticity state variable model to multiphase affirming that the interaction between coexisting phases is through an interface stress. We then employ a self-consistent polycrystalline model to help partition each individual phase's strain field, in a manner where a hybrid between compatibility and equilibrium is satisfied. With a synthesis of the aforementioned ideas, the additional TRIP is numerically accounted for by augmenting each flowrule with the computed interfacial stress. We are using a two-phase system and qualitatively associating these phases with martensite and austenite. The transformation kinetics proposed by Lusk [51, 72, 73], as well as some experimental data over a limited strain rate and tem-

perature regime were available to us. The goal of this is to eventually extend this work to all five phases in an attempt to modify and extend the approach taken by Bammann et al. [12–14,16]. The following mathematical operations in direct notation are used in the remainder of this paper. They are defined as follows. Given a second rank tensorial quantity $\mathbf{A}$, it follows that $\|\mathbf{A}\| = (\mathbf{A} : \mathbf{A})^{1/2}$, $Tr(\mathbf{A}) = (\mathbf{A} : \mathbf{I})^{1/2}$ and $\acute{\mathbf{A}} = \mathbf{A} - \frac{1}{3} Tr(\mathbf{A})\,\mathbf{I}$.

3.3 Methodology

3.3.1 On the Thermodynamics for Coexisting Phases

The formulation of the model follows the general thermodynamic formulation proposed by Bammann [17, 45]. The deformation or strain is decomposed into a lattice strain (which is further decomposed into strains in each component if multiple phases are present), the interface between phases, and the elastic strain associated with each defect densities in each phases. Therefore, given a body consisting of *n* phases, the strain components are:

$$\boldsymbol{\epsilon} \supset \left\{ \boldsymbol{\epsilon}_l^{(i)}, \boldsymbol{\epsilon}_{ss}^{(i)}, \boldsymbol{\epsilon}_\beta^{(i)}, \boldsymbol{\epsilon}_\pi \right\} \tag{3.3}$$

where $\boldsymbol{\epsilon}_l^{(i)}$ is the lattice strain in the each phase, $\boldsymbol{\epsilon}_{ss}^{(i)}$ is the strain resulting from statistically stored dislocations (SSDs) in the each phase, $\boldsymbol{\epsilon}_\beta^{(i)}$ is the strain resulting from geometrically necessary dislocations (GNDs) in the each phase, and $\boldsymbol{\epsilon}_\pi$ is the interface strain between phases. The symbol *i* ranges from 1 to the total number of phases *n* under consideration.

Furthermore, each of these strains is decomposed into elastic and inelastic or plastic parts, such that:

$$\boldsymbol{\epsilon}_{l}^{(i)} = \left(\boldsymbol{\epsilon}_{l,e}^{(i)} + \boldsymbol{\epsilon}_{l,p}^{(i)}\right) \qquad \boldsymbol{\epsilon}_{ss}^{(i)} = \left(\boldsymbol{\epsilon}_{ss,e}^{(i)} + \boldsymbol{\epsilon}_{ss,p}^{(i)}\right) \tag{3.4}$$

$$\boldsymbol{\epsilon}_{\beta}^{(i)} = \left(\boldsymbol{\epsilon}_{\beta,e}^{(i)} + \boldsymbol{\epsilon}_{\beta,p}^{(i)}\right) \qquad \boldsymbol{\epsilon}_{\pi} = \left(\boldsymbol{\epsilon}_{\pi,e} + \boldsymbol{\epsilon}_{\pi,p}\right) \tag{3.5}$$

From the second law of thermodynamics, the reduced entropy inequality is:

$$\dot{\psi} \leq W_{total} \tag{3.6}$$

where W_{total} represents the total work done. Similar to the thermodynamics proposed by Gurtin [42], for a single phase material the right hand side of the inequality represents the total work done comprising of macroscopic and microscopic:

$$\dot{\psi} \leq W_{macro} + W_{micro} \tag{3.7}$$

The composition of the macroscopic work is:

$$W_{macro} = \sum_{i=1}^{n} \boldsymbol{\sigma}^{(i)} : \left(\dot{\boldsymbol{\epsilon}}_{l}^{(i)} + \dot{\boldsymbol{\epsilon}}_{ss}^{(i)} + \dot{\boldsymbol{\epsilon}}_{\beta}^{(i)} + \dot{\boldsymbol{\epsilon}}_{\pi}\right) \tag{3.8}$$

where $\boldsymbol{\sigma}^{(i)}$ is the macroscopic Cauchy stress operating on each component of strain in a multiphase body. The microscopic work comprises of:

$$W_{micro} = \boldsymbol{\pi} : \dot{\boldsymbol{\epsilon}}_{\pi} + \sum_{i=1}^{n} \left[\boldsymbol{\kappa}^{(i)} : \left(\dot{\boldsymbol{\epsilon}}_{ss}^{(i)}\right) + \boldsymbol{\alpha}^{(i)} : \left(\dot{\boldsymbol{\epsilon}}_{\beta}^{(i)}\right)\right] \tag{3.9}$$

$\boldsymbol{\pi}$ is the tensorial interface stress between phases, $\boldsymbol{\kappa}^{(i)}$ is the tensorial stress like internal state variable serving as a work conjugate pair to the straining $\boldsymbol{\epsilon}_{ss}^{(i)}$ associated with the SSDs

in each phase and $\boldsymbol{\alpha}^{(i)}$ is the tensorial stress like internal state variable serving as a work conjugate pair to the straining $\boldsymbol{\epsilon}_{\beta}^{(i)}$ associated with the GNDs in each phase.

For now, we are going to assume at this time that $\boldsymbol{\epsilon}_{ss}^{(i)}$, the SSDs strain reduces to a scalar measure of the elastic strain in a dislocation array, which for a polycrysaline material averages to the same value in all directions, similar to the concept of isotropic hardening in classical plasticity. Similarly, we treat the interfacial stress in the same manner as the as acting in a non-directional manner. In a future work, we will utilize an orientation tensor to introduce the directionality of the tensorial interfacial π stress into the model, naturally incorporating the shearing aspects of the transformation process. In addition, we would neglect cross terms between stresses and strain rates. With this assumption, a given a body consisting of two phases, austenite and martensite, the macroscopic work simplifies to:

$$W_{macro} = \sum_{i=1}^{2} \boldsymbol{\sigma}^{(i)} : \left(\dot{\boldsymbol{\epsilon}}_{l}^{(i)}\right) \tag{3.10}$$

and the microscopic work reduces to:

$$W_{micro} = \pi \dot{\epsilon}_{\pi} + \sum_{i=1}^{2} \left[\kappa^{(i)} \left(\dot{\epsilon}_{ss}^{(i)}\right) + \boldsymbol{\alpha}^{(i)} : \left(\dot{\boldsymbol{\epsilon}}_{\beta}^{(i)}\right)\right] \tag{3.11}$$

Following the approach introduced by Coleman and Noll [25] in an attempt to determine the logical connection between the principles of conservation of energy, entropy inequality and the general principles in mechanics, Coleman and Gurtin [23] determined the thermodynamic restrictions necessary when introducing ISVs to a continuum mechanics framework. In the same light we argue that, the Helmholtz free energy is of the form:

$$\psi = e - \theta\eta \tag{3.12}$$

where e is the internal energy, θ represents temperature and η the entropy. In rate form the Helmholtz free energy is:

$$\dot{\psi} = \dot{e} - \dot{\theta}\eta - \theta\dot{\eta} \tag{3.13}$$

If we assume isothermal conditions, the rate form of the Helmholtz free energy reduces to:

$$\dot{\psi} = \dot{e} - \theta\dot{\eta} \tag{3.14}$$

Substituting Eqn. (3.10) and Eqn. (3.11) into Eqn. (3.7) gives:

$$\dot{\psi} \leq \sum_{i=1}^{2} \boldsymbol{\sigma}^{(i)} : \left(\dot{\boldsymbol{\epsilon}}_{l}^{(i)}\right) + \pi\dot{\epsilon}_{\pi} + \sum_{i=1}^{2} \left[\kappa^{(i)} \left(\dot{\epsilon}_{ss}^{(i)}\right) + \boldsymbol{\alpha}^{(i)} : \left(\dot{\boldsymbol{\epsilon}}_{\beta}^{(i)}\right)\right] \tag{3.15}$$

Furthermore, decomposing each of these strains into elastic and inelastic or plastic parts, Eqn. (3.15) becomes:

$$\begin{aligned} \dot{\psi} \quad &\leq \quad \pi\left(\dot{\epsilon}_{\pi,e} + \dot{\epsilon}_{\pi,p}\right) + \sum_{i=1}^{2} \boldsymbol{\sigma}^{(i)} : \left(\dot{\boldsymbol{\epsilon}}_{l,e}^{(i)} + \dot{\boldsymbol{\epsilon}}_{l,p}^{(i)}\right) \\ &+ \quad \sum_{i=1}^{2} \left[\kappa^{(i)} \left(\dot{\epsilon}_{ss,e}^{(i)} + \dot{\epsilon}_{ss,p}^{(i)}\right) + \boldsymbol{\alpha}^{(i)} : \left(\dot{\boldsymbol{\epsilon}}_{\beta,e}^{(i)} + \dot{\boldsymbol{\epsilon}}_{\beta,p}^{(i)}\right)\right] \end{aligned} \tag{3.16}$$

Assuming that no inelastic deformation occurs, at the interface, Eqn. (3.16) becomes:

$$\begin{aligned} \dot{\psi} \quad &\leq \quad \pi\left(\dot{\epsilon}_{\pi,e}\right) + \sum_{i=1}^{2} \boldsymbol{\sigma}^{(i)} : \left(\dot{\boldsymbol{\epsilon}}_{l,e}^{(i)} + \dot{\boldsymbol{\epsilon}}_{l,p}^{(i)}\right) \\ &+ \quad \sum_{i=1}^{2} \left[\kappa^{(i)} \left(\dot{\epsilon}_{ss,e}^{(i)} + \dot{\epsilon}_{ss,p}^{(i)}\right) + \boldsymbol{\alpha}^{(i)} : \left(\dot{\boldsymbol{\epsilon}}_{\beta,e}^{(i)} + \dot{\boldsymbol{\epsilon}}_{\beta,p}^{(i)}\right)\right] \end{aligned} \tag{3.17}$$

We assume that the Helmholtz free energy depends on a number of independent state variables namely the elastic portion of the lattice strain in each phase $\boldsymbol{\epsilon}_{l,e}^{(i)}$, the elastic strain like internal state variable due to SSD and GNDs $\epsilon_{ss,e}^{(i)}$ and $\boldsymbol{\epsilon}_{\beta,e}^{(i)}$ and the elastic interfacial strain $\epsilon_{\pi,e}$. We further represent each category of state variables in each phase as:

$$\mathbf{Z}_{l,e} \Rightarrow \left\{\boldsymbol{\epsilon}_{l,e}^{(1)}, \boldsymbol{\epsilon}_{l,e}^{(2)}\right\} \qquad Z_{ss,e} \Rightarrow \left\{\epsilon_{ss,e}^{(1)}, \epsilon_{ss,e}^{(2)}\right\} \tag{3.18}$$

$$\mathbf{Z}_{\beta,e} \Rightarrow \left\{\boldsymbol{\epsilon}_{\beta,e}^{(1)}, \boldsymbol{\epsilon}_{\beta,e}^{(2)}\right\} \qquad \epsilon_{\pi,e} \tag{3.19}$$

Therefore the Helmholtz free energy is further expressed as dependent on:

$$\psi = \hat{\psi}\left(\mathbf{Z}_{l,e}, Z_{ss,e}, \mathbf{Z}_{\beta,e}, \epsilon_{\pi,e}\right) \tag{3.20}$$

Applying the chain rule to Eqn. (3.20) yields:

$$\dot{\psi} = \sum_{i=1}^{2} \frac{\partial \psi}{\partial \boldsymbol{\epsilon}_{l,e}^{(i)}} : \dot{\boldsymbol{\epsilon}}_{l,e}^{(i)} + \sum_{i=1}^{2} \frac{\partial \psi}{\partial \epsilon_{ss,e}^{(i)}} \dot{\epsilon}_{ss,e}^{(i)} + \sum_{i=1}^{2} \frac{\partial \psi}{\partial \boldsymbol{\epsilon}_{\beta,e}^{(i)}} : \dot{\boldsymbol{\epsilon}}_{\beta,e}^{(i)} + \frac{\partial \psi}{\partial \epsilon_{\pi,e}} \dot{\epsilon}_{\pi,e} \tag{3.21}$$

Substituting Eqn. (3.21) into Eqn. (3.17) and further expanding:

$$\begin{aligned}
\frac{\partial \psi}{\partial \boldsymbol{\epsilon}_{l,e}^{(1)}} : \dot{\boldsymbol{\epsilon}}_{l,e}^{(1)} + \frac{\partial \psi}{\partial \boldsymbol{\epsilon}_{l,e}^{(2)}} : \dot{\boldsymbol{\epsilon}}_{l,e}^{(2)} + \frac{\partial \psi}{\partial \epsilon_{ss,e}^{(1)}} \dot{\epsilon}_{ss,e}^{(1)} + \frac{\partial \psi}{\partial \epsilon_{ss,e}^{(2)}} \dot{\epsilon}_{ss,e}^{(2)} \quad + \\
\frac{\partial \psi}{\partial \boldsymbol{\epsilon}_{\beta,e}^{(1)}} : \dot{\boldsymbol{\epsilon}}_{\beta,e}^{(1)} + \frac{\partial \psi}{\partial \boldsymbol{\epsilon}_{\beta,e}^{(2)}} : \dot{\boldsymbol{\epsilon}}_{\beta,e}^{(2)} + \frac{\partial \psi}{\partial \epsilon_{\pi,e}} \dot{\epsilon}_{\pi,e} \quad \leq \\
\boldsymbol{\sigma}^{(1)} : \left(\dot{\boldsymbol{\epsilon}}_{l,e}^{(1)} + \dot{\boldsymbol{\epsilon}}_{l,p}^{(1)}\right) + \boldsymbol{\sigma}^{(2)} : \left(\dot{\boldsymbol{\epsilon}}_{l,e}^{(2)} + \dot{\boldsymbol{\epsilon}}_{l,p}^{(2)}\right) \quad + \\
\boldsymbol{\alpha}^{(1)} : \left(\dot{\boldsymbol{\epsilon}}_{\beta,e}^{(1)} + \dot{\boldsymbol{\epsilon}}_{\beta,p}^{(1)}\right) + \boldsymbol{\alpha}^{(2)} : \left(\dot{\boldsymbol{\epsilon}}_{\beta,e}^{(2)} + \dot{\boldsymbol{\epsilon}}_{\beta,p}^{(2)}\right) \quad + \\
\kappa^{(1)}\left(\dot{\epsilon}_{ss,e}^{(1)} + \dot{\epsilon}_{ss,p}^{(1)}\right) + \kappa^{(2)}\left(\dot{\epsilon}_{ss,e}^{(2)} + \dot{\epsilon}_{ss,p}^{(2)}\right) + \pi\left(\dot{\epsilon}_{\pi,e}\right)
\end{aligned} \tag{3.22}$$

Employing the Coleman and Noll [25] argument and grouping yields:

$$\begin{aligned}
(\frac{\partial \psi}{\partial \boldsymbol{\epsilon}_{l,e}^{(1)}} - \boldsymbol{\sigma}^{(1)}) : \dot{\boldsymbol{\epsilon}}_{l,e}^{(1)} + (\frac{\partial \psi}{\partial \boldsymbol{\epsilon}_{l,e}^{(2)}} - \boldsymbol{\sigma}^{(2)}) : \dot{\boldsymbol{\epsilon}}_{l,e}^{(2)} \quad + \\
(\frac{\partial \psi}{\partial \boldsymbol{\epsilon}_{\beta,e}^{(1)}} - \boldsymbol{\alpha}^{(1)}) : \dot{\boldsymbol{\epsilon}}_{\beta,e}^{(1)} + (\frac{\partial \psi}{\partial \boldsymbol{\epsilon}_{\beta,e}^{(2)}} - \boldsymbol{\alpha}^{(2)}) : \dot{\boldsymbol{\epsilon}}_{\beta,e}^{(2)} \quad + \\
(\frac{\partial \psi}{\partial \epsilon_{ss,e}^{(1)}} - \kappa^{(1)})\dot{\epsilon}_{ss,e}^{(1)} + (\frac{\partial \psi}{\partial \epsilon_{ss,e}^{(2)}} - \kappa^{(2)})\dot{\epsilon}_{ss,e}^{(2)} \quad + \\
(\frac{\partial \psi}{\partial \epsilon_{\pi,e}} - \pi)\dot{\epsilon}_{\pi,e} \quad \leq \\
\boldsymbol{\sigma}^{(1)} : \left(\dot{\boldsymbol{\epsilon}}_{l,p}^{(1)}\right) + \boldsymbol{\sigma}^{(2)} : \left(\dot{\boldsymbol{\epsilon}}_{l,p}^{(2)}\right) + \boldsymbol{\alpha}^{(1)} : \left(\dot{\boldsymbol{\epsilon}}_{\beta,p}^{(1)}\right) + \boldsymbol{\alpha}^{(2)} : \left(\dot{\boldsymbol{\epsilon}}_{\beta,p}^{(2)}\right) \quad + \\
\kappa^{(1)}\left(\dot{\epsilon}_{ss,p}^{(1)}\right) + \kappa^{(2)}\left(\dot{\epsilon}_{ss,p}^{(2)}\right)
\end{aligned} \tag{3.23}$$

Therefore as the elastic strains vanish:

$$\boldsymbol{\sigma}^{(1)} = \frac{\partial \psi}{\partial \boldsymbol{\epsilon}_{l,e}^{(1)}} \qquad \boldsymbol{\sigma}^{(2)} = \frac{\partial \psi}{\partial \boldsymbol{\epsilon}_{l,e}^{(2)}} \tag{3.24}$$

$$\boldsymbol{\alpha}^{(1)} = \frac{\partial \psi}{\partial \boldsymbol{\epsilon}_{\alpha,e}^{(1)}} \qquad \boldsymbol{\alpha}^{(2)} = \frac{\partial \psi}{\partial \boldsymbol{\epsilon}_{\alpha,e}^{(2)}} \tag{3.25}$$

$$\kappa^{(1)} = \frac{\partial \psi}{\partial \dot{\epsilon}_{ss,e}^{(2)}} \qquad \kappa^{(2)} = \frac{\partial \psi}{\partial \dot{\epsilon}_{ss,e}^{(2)}} \tag{3.26}$$

$$\pi = \frac{\partial \psi}{\partial \epsilon_{\pi,e}} \tag{3.27}$$

The dissipation inequality becomes:

$$\boldsymbol{\sigma}^{(1)} : \left(\dot{\boldsymbol{\epsilon}}_{l,p}^{(1)}\right) + \boldsymbol{\sigma}^{(2)} : \left(\dot{\boldsymbol{\epsilon}}_{l,p}^{(2)}\right) + \boldsymbol{\alpha}^{(1)} : \left(\dot{\boldsymbol{\epsilon}}_{\beta,p}^{(1)}\right) + \boldsymbol{\alpha}^{(2)} : \left(\dot{\boldsymbol{\epsilon}}_{\beta,p}^{(2)}\right) \quad + \\ \kappa^{(1)} \left(\dot{\epsilon}_{ss,p}^{(1)}\right) + \kappa^{(2)} \left(\dot{\epsilon}_{ss,p}^{(2)}\right) \geq 0 \tag{3.28}$$

The internal state variables $\kappa^{(i)}$ and $\boldsymbol{\alpha}^{(i)}$ are chosen to be of the form:

$$\kappa^{(i)} = 2\mu^{(i)} C_{\kappa}^{(i)} \epsilon_{ss}^{(i)} \tag{3.29}$$

and

$$\boldsymbol{\alpha}^{(i)} = 2\mu^{(i)} C_{\alpha}^{(i)} \boldsymbol{\epsilon}_{\beta}^{(i)} \tag{3.30}$$

where $\mu^{(i)}$ is the temperature dependent shear modulus, $\epsilon_{ss}^{(i)}$ and $\epsilon_{\beta}^{(i)}$ are the straining associated with the SSDs and GNDs and $C_{\kappa}^{(i)}$ and $C_{\alpha}^{(i)}$ are dimensionless material parameters associated with each phase.

The stress like internal state variable $\kappa^{(i)}$, the work conjugate variable to the straining $\epsilon_{ss}^{(i)}$ associated with the SSDs in each phase. The mathematical definition of $\epsilon_{ss}^{(i)}$ in each phase is:

$$\epsilon_{ss}^{(i)} = b^{(i)} \sqrt{\rho_{ss}^{(i)}} \tag{3.31}$$

where $b^{(i)}$ is the magnitude of the burger and $\rho_{ss}^{(i)}$ is the dislocation density of SSDs. The rate form the SSDs density is:

$$\dot{\epsilon}_{ss}^{(i)} = \frac{b^{(i)}}{2} \frac{1}{\sqrt{\rho_{ss}^{(i)}}} \dot{\rho}_{ss}^{(i)} \tag{3.32}$$

The form of the evolution law for $\dot{\rho}_{ss}^{(i)}$ as determined by Kock and Mecking [53] and Estrin and Mecking [31] accounting for thermally activated hardening and dynamic recovery of SSDs, in each phase is:

$$\dot{\rho}_{ss}^{(i)} = \left(c_1^{(i)} \sqrt{\rho_{ss}^{(i)}} - c_2^{(i)} \left(\theta\right) \rho_{ss}^{(i)} \right) \dot{\epsilon}_p^{eff} \tag{3.33}$$

where $\dot{\epsilon}_p^{(i)}$ is the effective plastic strain rate in each phase. $c_1^{(i)}$ and $c_2^{(i)}$ are material parameters for each phase determined using experimental data. The static recovery component of $\dot{\rho}_{ss}^{(i)}$ accounting for thermal diffusion of dislocations as determined by Nes [85] is of the form of the:

$$\dot{\rho}_{ss}^{(i)} = -c_3^{(i)} \left(\theta\right) \rho_{ss}^{(i)} \sinh \left[c_4^{(i)} \left(\theta\right) \sqrt{\rho_{ss}^{(i)}} \right] \tag{3.34}$$

where $c_3^{(i)}$ and $c_4^{(i)}$ are material parameters for each phase determined using experimental data. In full form, the SSDs density rate $\dot{\rho}_{ss}^{(i)}$ accounting for thermal diffusion of dislocations and thermally activated hardening and dynamic recovery is:

$$\dot{\rho}_{ss}^{(i)} = \left(c_1^{(i)} \sqrt{\rho_{ss}^{(i)}} - c_2^{(i)} \left(\theta\right) \rho_{ss}^{(i)} \right) \dot{\epsilon}_p^{(i)} - c_3^{(i)} \left(\theta\right) \rho_{ss}^{(i)} \sinh \left[c_4^{(i)} \left(\theta\right) \sqrt{\rho_{ss}^{(i)}} \right] \tag{3.35}$$

Substituting Eqn. (3.29), Eqn. (3.31) and Eqn. (3.32) into Eqn. (3.35) gives the evolution equation for κ (Eqn. (2.18)):

$$\begin{aligned} \dot{\kappa}^{(i)} &= \frac{\kappa^{(i)}}{\mu^{(i)}} \left(\frac{d\mu}{d\theta}\right)^{(i)} \dot{\theta}^{(i)} + 2\mu^{(i)} H^{(i)} C_k^{(i)} \dot{\epsilon}_p^{(i)} \\ &- R_d^{(i)} \kappa^{(i)} \dot{\epsilon}_p^{(i)} - R_s^{(i)} \kappa^{(i)} \sinh \left[\frac{Q_s^{(i)} \kappa^{(i)}}{2\mu^{(i)} C_k^{(i)}} \right] \end{aligned} \tag{3.36}$$

The evolution law for the tensorial internal state variable $\boldsymbol{\alpha}^{(i)}$ in each phase, is chosen to be in a hardening minus recovery format following Armstrong and Frederick [34]:

$$\dot{\boldsymbol{\epsilon}}_{\beta}^{(i)} = \left(h^{(i)}\mathbf{N}^{(i)} - rd^{(i)}\sqrt{\frac{2}{3}}\boldsymbol{\epsilon}_{\beta}^{(i)} \quad \boldsymbol{\epsilon}_{\beta}^{(i)} \right) \dot{\epsilon}_{p}^{(i)} \tag{3.37}$$

Substituting Eqn. (3.30) into Eqn. (3.37) gives the evolution equation for $\boldsymbol{\alpha}$ (Eqn. (2.16)):

$$\begin{aligned} \mathring{\boldsymbol{\alpha}}^{(i)} &= \frac{\boldsymbol{\alpha}^{(i)}}{\mu^{(i)}}\left(\frac{d\mu}{d\theta}\right)^{(i)}\dot{\theta}^{(i)} + 2\mu^{(i)}h^{(i)}C_a^{(i)}\sqrt{\frac{3}{2}}\mathbf{d}_p^{(i)} \\ &- \frac{r_d^{(i)}}{2\mu^{(i)}C_a^{(i)}}\sqrt{\frac{2}{3}}\dot{\epsilon}_p^{(i)} \quad \boldsymbol{\alpha}^{(i)} \quad \boldsymbol{\alpha}^{(i)} \end{aligned} \tag{3.38}$$

where the convective derivative of $\boldsymbol{\alpha}$ is of the form (Eqn. (2.17)):

$$\mathring{\boldsymbol{\alpha}}^{(i)} = \dot{\boldsymbol{\alpha}}^{(i)} - \mathbf{w}_e^{(i)}\boldsymbol{\alpha}^{(i)} + \boldsymbol{\alpha}^{(i)}\mathbf{w}_e^{(i)} \tag{3.39}$$

3.3.2 On the Transformation Kinetics Model

The final set of equations needed to complete the multiphase model is the phase transformation kinetic evolution equation. Transformation kinetic models are evolution equations that physically dictate the time rate of each phase. Under considering here is two phases, qualitatively associated with austenite to martensite. There the transformation equation considered are of a non-diffusion type. To date the KM [56] model is the most widely adopted kinetics transformation model used for capturing austenite to martensite transformation. The KM model is given by:

$$\dot{\phi} = -b_{km}\exp[-b_{km}(M_s - \theta)]U(\theta)\dot{\theta} \tag{3.40}$$

where b_{km} is a fixed parameter. θ_{start} is the temperature at the start of martensite formation. $U[\theta]$ is a unit step function given by:

$$U(\theta) = \begin{cases} 1 & M_f \leq \theta \leq M_s \\ 0 & else \end{cases} \tag{3.41}$$

where M_s and M_f are martensite start and finish temperature. For many reasons not limited to the notable burst in transformation rate analogous to a mathematical discontinuity, it has become necessary to develop alternative models. Figure 3.1 shows the commonly referred to sharp transient in transformation rate as alluded to by [87]. The KM model was evaluated at carbon content %C = 0.1,0,2,0.3,0.4 at a fixed cooling rate.

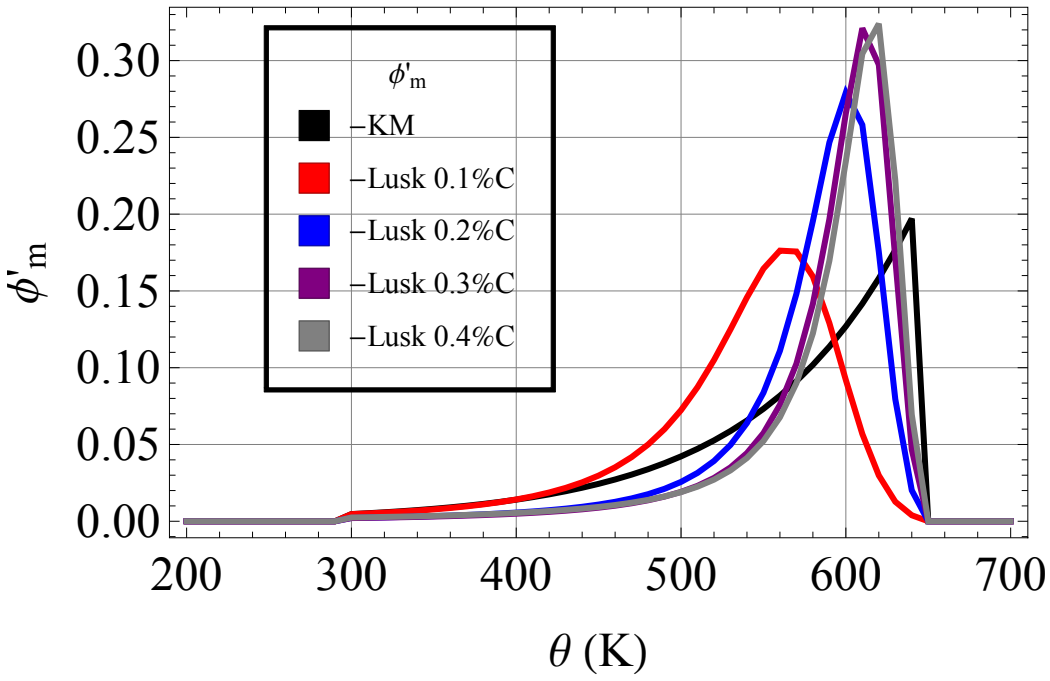

Figure 3.1

Kinetics rate using Lusk and KM model at carbon content %C = 0.1,...,0.4.

The KM model has an explicit dependence on the rate of change of temperature and a fixed parameter $b_{km} = 0.011$. In other to circumvent the burst in transformation rate of the modeled martensitic formation experienced when using the KM model, new models have been developed. These models are analogous in part to the transformation profile but with less of a discontinuous transformation rate. The non-diffusional kinetics model adopted here is that of Lusk et al. [51, 72, 73] where additional consideration was given to the carbon content influence on the transformation rate. Using the Lusk model, austenite's phase fraction ($\phi^{(1)}$) is determined using:

$$\frac{d\phi^{(1)}}{dt} = -\frac{d\phi^{(2)}}{dt} \tag{3.42}$$

The initial conditions for the austenitic phase is such that:

$$\phi^{(1)}(t_0) = 0.99999 \tag{3.43}$$

For the evolution of martensite phase we have that:

$$\frac{d\phi^{(2)}}{dt} = -v(\%C)\left(\phi^{(2)}\right)^{a(\%C)}\left(1-\phi^{(2)}\right)^{b(\%C)} U(\theta)\frac{d\theta}{dt} \tag{3.44}$$

where $\%C$ is the carbon content in percentage. $\dot{\theta}$ is the temprature rate. *v*, *a*, and *b* are transformation parameters fit to dilatometry test. Marteniste start M_s temperature was determined using Andrews [2] formula where the material chemistry is the sole determining factor. The form of the parameters *v*:

$$v(\%C) = v_0 + v_1\%C + v_2\%C^2 + v_3\%C^3 \tag{3.45}$$

The form of the parameters *a*:

$$a(\%C) = a_0 + a_1\%C \tag{3.46}$$

The form of the parameters b is:

$$b\,(\%C) = b_0 + b_1 \%C \tag{3.47}$$

The initial condition for the martensitic phase is given by:

$$\phi^{(2)}\,(t_0) = 0.00001 \tag{3.48}$$

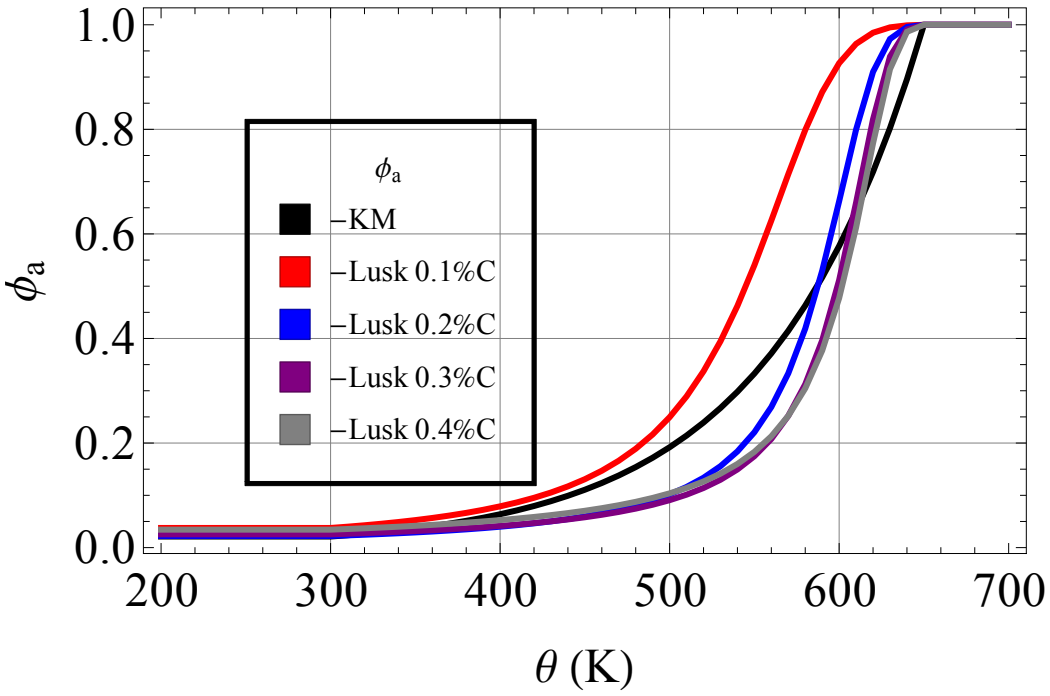

Figure 3.2

Lusk model at a fixed cooling rate evaluated at %C = 0.1,0.2,0.3,0.4.

Independent of the mechanical response Figure 3.2 shows the carbon content influence on the transformation kinetics for any given cooling rate. The cooling rate serves as a driving function for the transformation kinetics. Specifically, it is a is a linear multiple of

the volume fraction at each time step. For these cases M_s was chosen to be fixed, however, based on the Andrews [2] formula this is not the case. There is a variation due to the carbon content influence.

3.3.3 Integration of the Multiphase EMMI Constitutive Equations

To numerically integrate the constitutive multiphase EMMI model equations Eqn. (2.4-3.44) we make the assumption that the discretized set of equations sufficiently satisfy the continuous form; to a prescribed level of accuracy determined by the integration scheme. The multiphase EMMI model is further cast into a discrete form with the symbol *n+1* and *n* indicating the current and previous time step solutions, respectively. Table 3.1 is the direct integration algorithm for the constitutive EMMI model equations. The algorithms is suitable for any specified strain rate or temperature. An explicit Euler finite difference scheme is used for the time integration of the stress and state variables in each phase. The incremental form of the elastic asymmetrical portion of the velocity gradient in each phase is:

$$\Delta \mathbf{w}_e^{(i)} = \Delta \mathbf{w}^{(i)} - \Delta \mathbf{w}_p^{(i)} - \Delta \mathbf{w}_\theta^{(i)}. \tag{3.49}$$

Similarly the incremental form of the symmetrical portion of the velocity gradient in each phase is:

$$\Delta \mathbf{d}_e^{(i)} = \Delta \mathbf{d}^{(i)} - \Delta \mathbf{d}_p^{(i)} - \Delta \mathbf{d}_\theta^{(i)}. \tag{3.50}$$

The incremental form of the plastic part of the symmetrical portion of the velocity gradient in each phase is computed using:

$$\Delta \mathbf{d}_p^{(i)} = \sqrt{\frac{3}{2}} \Delta \epsilon_p^{(i)} \acute{\mathbf{N}}^{(i),n+1} \tag{3.51}$$

where $\acute{\mathbf{N}}^{(i),n+1}$ is the direction of the plastic flow given by:

$$\acute{\mathbf{N}}^{(i),n+1} = \frac{\acute{\boldsymbol{\xi}}^{(i),n+1}}{\acute{\boldsymbol{\xi}}^{(i),n+1}}. \tag{3.52}$$

The norm of the net effective stress is given by:

$$\acute{\boldsymbol{\xi}}^{(i),n+1} \;=\; \acute{\boldsymbol{\sigma}}^{(i),n+1} - \frac{2}{3}\boldsymbol{\alpha}^{(i),n+1} \tag{3.53}$$

$\Delta\epsilon_p^{(i)}$ is the incremental form of net effective plastic flow in each phase which can be evaluated using several approaches. For an explicit Euler algorithm, $\Delta\epsilon_p^{(i)}$ depends on the previous time step values of the stress and internal state variables in each phase. With this observation, $\Delta\epsilon_p^{(i)}$ can be simply computed using a functional evaluation approach. Using a simple functional evaluation, $\Delta\epsilon_p^{(i)}$ is computed and stored as:

$$\Delta\epsilon_p^{(i)} = f^{(i)} \sinh\left[\frac{\sqrt{\frac{3}{2}}\;\; \Delta\acute{\boldsymbol{\xi}}^{(i),n} \;\; \pm \pi^{(i),n+1}}{\Delta\kappa^{(i),n} + Y^{(i)}} - 1\right]^{n^{(i)}} \tag{3.54}$$

An incremental approach can be used to compute the incremental net effective plastic flow ($\Delta\epsilon_p^{(i)}$) in each phase. This approach requires mathematically treating the net effective plastic flow as an ordinary differential equation (ODE). As an ODE, the current time step value of the plastic strain $\epsilon_p^{(i),n+1}$ in each phase to be computed using the previous time step value $\epsilon_p^{(i),n}$. This implies that:

$$\epsilon_p^{(i),n+1} = \epsilon_p^{(i),n} + f^{(i)} \sinh\left[\frac{\sqrt{\frac{3}{2}}\;\; \Delta\acute{\boldsymbol{\xi}}^{(i),n} \;\; \pm \pi^{(i),n+1}}{\Delta\kappa^{(i),n} + Y^{(i)}} - 1\right]^{n^{(i)}} \tag{3.55}$$

The incremental $\Delta\epsilon_p^{(i)}$ is needed in order to calculate the stress and internal state variables in each phase at the current time level $n+1$. The incremental value of the net effective plastic flow $\Delta\epsilon_p^{(i)}$ in each phase is:

$$\Delta\epsilon_p^{(i)} = \epsilon_p^{(i),n+1} - \epsilon_p^{(i),n}. \tag{3.56}$$

Figure 3.3 shows EMMI model response to uniaxial tension using a functional versus an incremental evaluation approach to evaluating $\Delta\epsilon_p^{(i)}$ using SS304L at strain rate of $\dot{\epsilon} = 0.1/s$. The results show no distinction between both methods. The difference in computational cost is also negligible; depending on implementation into computer code.

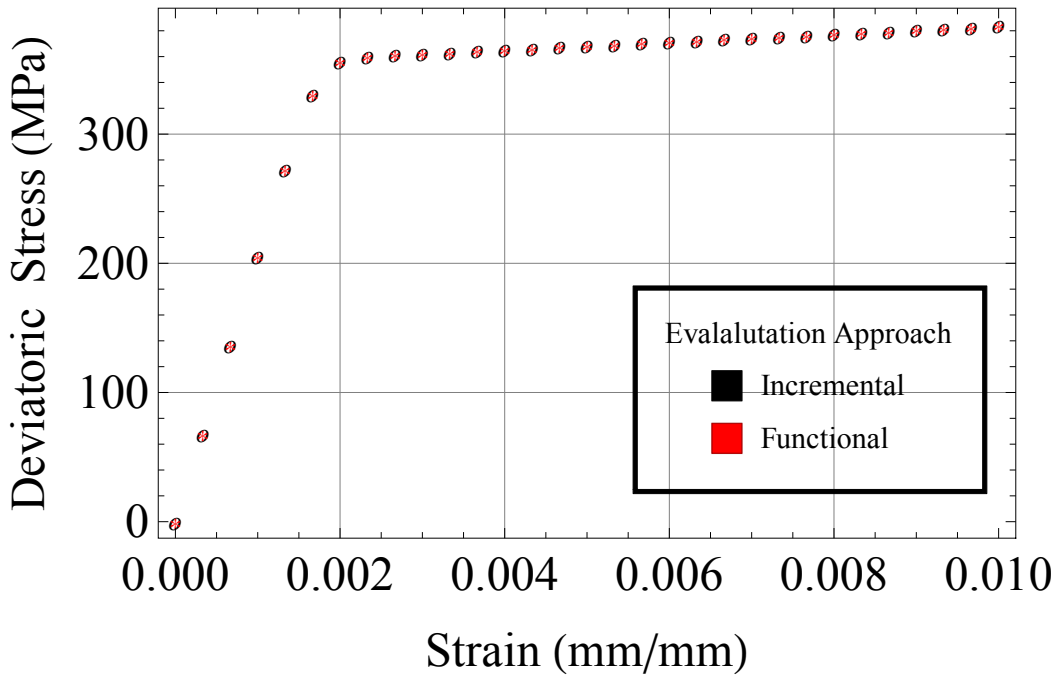

Figure 3.3

Functional vs. an incremental approach for SS304L at $\dot{\epsilon} = 0.1/s$

The incremental form of the thermal part of the symmetrical portion of the velocity gradient in each phase is computed using:

$$\Delta \mathbf{d}_{\theta}^{(i)} = \Delta \epsilon_{\theta}^{(i)} \mathbf{I} \tag{3.57}$$

where the incremental thermal strain is:

$$\Delta \epsilon_{\theta}^{(i)} = f_{\beta}(\theta^n)^{(i)} \Delta \theta. \tag{3.58}$$

$f_{\beta}(\theta^n)^{(i)}$ is the form of the temperature dependence of the coefficient of thermal expansion given by:

$$f_{\beta}(\theta^n)^{(i)} = \frac{\beta(\theta^n)^{(i)} - \beta_0^{(i)} b_{\theta}^{(i)} (\theta^n - \theta_0)}{(1 - \beta(\theta^n)^{(i)} (\theta^n - \theta_0))} \tag{3.59}$$

where $b_{\theta}^{(i)}$ is a coefficient of thermal expansion parameter. The form of $\beta_0^{(i)}$ is given by:

$$\beta(\theta^n)^{(i)} = \beta_0^{(i)} (1 - b_{\theta}^{(i)} (\theta^n - \theta_0)) \tag{3.60}$$

The incremental form of the isotropic hardening evolution equation yield:

$$\begin{aligned} \kappa^{(i),n+1} &= \kappa^{(i),n} + \kappa^{(i),n} (\mu^{(i)})^{-1} \Delta \mu^{(i)} \\ &+ (2\mu^{(i)} H^{(i)} C_k^{(i)} - R_d^{(i)} \kappa^{(i),n}) \Delta \epsilon_p^{(i)} \\ &- \Delta t R_s^{(i)} \kappa^{(i),n} \sinh \left[\kappa^{(i),n} Q_s^{(i)} (2 C_k^{(i)} \mu^{(i)})^{-2} \right] \end{aligned} \tag{3.61}$$

where all material parameters and constants are evaluated at the prescribe temperature. The incremental form of the kinematic hardening evolution equation is such that:

$$\begin{aligned} \boldsymbol{\alpha}^{(i),n+1} &= \boldsymbol{\alpha}^{(i),n} + \boldsymbol{\alpha}^{(i),n} (\mu^{(i)})^{-1} \Delta \mu^{(i)} \\ &+ 2\mu^{(i)} h^{(i)} C_a^{(i)} \sqrt{\frac{3}{2}} \Delta \epsilon_p^{(i)} \mathbf{N}^{(i),n} \\ &- \frac{r_d^{(i)}}{2\mu^{(i)} C_a^{(i)}} \sqrt{\frac{2}{3}} \Delta \epsilon_p^{(i)} \quad \boldsymbol{\alpha}^{(i),n} \quad \boldsymbol{\alpha}^{(i),n} \\ &+ \Delta \mathbf{w}_e^{(i)} \boldsymbol{\alpha}^{(i),n} - \boldsymbol{\alpha}^{(i),n} \Delta \mathbf{w}_e^{(i)}. \end{aligned} \tag{3.62}$$

The incremental form of the deviatoric Cauchy stress is given by:

$$\begin{aligned}\mathbf{s}^{(i),n+1} &= \mathbf{s}^{(i),n} + \mathbf{s}^{(i),n}(\mu^{(i)})^{-1}\Delta\mu^{(i)} \\ &+ \Delta t 2\mu^{(i)}\Delta\acute{\mathbf{d}}_e^{(i),n} \\ &+ \Delta\mathbf{w}_e^{(i),n}\mathbf{s}^{(i),n} - \mathbf{s}^{(i),n}\Delta\mathbf{w}_e^{(i),n}. \end{aligned} \tag{3.63}$$

The incremental form of the pressure is such that:

$$\begin{aligned}\mathbf{p}^{(i),n+1} &= \mathbf{p}^{(i),n} + \mathbf{p}^{(i),n}(K^{(i)})^{-1}\Delta K^{(i)} \\ &+ \Delta t K^{(i)} Tr[\Delta\mathbf{d}_e^{(i),n}] \\ &+ \Delta\mathbf{w}_e^{(i),n}\mathbf{p}^{(i),n} - \mathbf{p}^{(i),n}\Delta\mathbf{w}_e^{(i),n}. \end{aligned} \tag{3.64}$$

The incremental form of the interfacial stress evolution equation is such that:

$$\boldsymbol{\pi}^{n+1} = \boldsymbol{\pi}^n + C_\pi \frac{\Delta V}{V^{n+1}} \left[1 - 2\phi^{n+1}\right] \Delta\phi \tag{3.65}$$

$\frac{\Delta V}{V^{n+1}}$ is the volume change due to carbon content variation given by:

$$\Delta V = V^{n+1} - V^n \tag{3.66}$$

where the volume at the current and previous time steps are computed using:

$$V^{n+1} = 3.548 + 0.44\%C^{n+1} \qquad V^n = 3.548 + 0.44\%C^n \tag{3.67}$$

The incremental form of the volume fraction of martensite is such that:

$$\phi^{n+1} = \phi^n - \left[v(\phi^n)^a(1-\phi^n)^b U\right] \Delta\theta \tag{3.68}$$

where the incremental temperature difference ($\Delta\theta$) is computed using:

$$\Delta\theta = \theta^{n+1} - \theta^n \tag{3.69}$$

Using the discretized set of equations, the multiphase EMMI model equations are integrated directly (Table 3.2). Classical algorithms are designed around a yield surface, however, direct integration of the multiphase EMMI model utilizes a functional argument determined by the kernel of the flowrule. The argument is such that plastic flow occurs iff:

$$\sqrt{\frac{3}{2}}\frac{\mathbf{s}-\frac{2}{3}\boldsymbol{\alpha}\ \ \pm\pi}{(\kappa+Y)}>1 \tag{3.70}$$

otherwise the stress and internal state variables in each phase retain their previous time step values. For a purely explicit algorithm, the current time step value for the stress can be computed for each phase. However, for the internal state variables in each phase only the previous time value is available. Therefore, the discrete form of Eqn. (3.70) for a purely explicit algorithm is such that:

$$\sqrt{\frac{3}{2}}\frac{\mathbf{s}^{(i),n+1}-\frac{2}{3}\boldsymbol{\alpha}^{(i),n}\ \ \pm\pi}{(\kappa^{(i),n}+Y)}>1. \tag{3.71}$$

3.4 Results

A quantitative assessment of the multiphase EMMI material model coupled with the non-diffusive phase transformation kinetic model of Lusk et al. [51,72,73] was carried out. Parameter identification for the mechanical response of both the austenite and martensite phases was performed using a gradient based optimization routine as listed on Table 2.1 following previous works of Marin et al. [80]. Table 2.2 is a tabulation of the material properties used in this study. Parameters used here for the kinetic models are published values based on previous works of Lusk et al. [51, 72, 73]. For the sake of simplicity material hardening dependence on carbon content was not accounted for. Figure 3.4 and

Table 3.1

Direct Integration Algorithm for Single Phase EMMI Model

Step 0:	Compute Material Parameters
Step 1:	At Time = 0, Material Initialization Procedure
$\Rightarrow$	Compute: $\Delta\boldsymbol{\epsilon}$ or $\Delta\mathbf{d}$
$\Rightarrow$	Compute $\boldsymbol{\sigma}^1$
$\Rightarrow$	Retrieve and Store $\boldsymbol{\alpha}^0$, κ^0 and $\Delta\boldsymbol{\epsilon}_p^0$
Step 2:	At Time $>$ 0, Material Integration Procedure
$\Rightarrow$	Compute: $\Delta\epsilon$ and $\Delta\mathbf{d}$
$\Rightarrow$	Retrieve: $\boldsymbol{\sigma}^n$, $\boldsymbol{\alpha}^n$, κ^n and $\Delta\boldsymbol{\epsilon}_p^n$
$\Rightarrow$	Compute: $\boldsymbol{\sigma}^{n+1}$
$\Rightarrow$	Decompose $\boldsymbol{\sigma}^{n+1}$ into $\mathbf{s}^{n+1}$ and $\mathbf{p}^{n+1}$
$\Rightarrow$	Determine magnitude of plastic deformation :
$\Rightarrow$	Evaluate: $\sqrt{\frac{3}{2}}\ \left\|\mathbf{s}^{n+1} - \frac{2}{3}\boldsymbol{\alpha}^n\right\| > (\kappa^n + Y)$
	If(True) $\Rightarrow$ Evaluate: $\Delta\boldsymbol{\epsilon}_p$ or $\Delta\mathbf{d}_p$ $\Rightarrow$ Compute: $\boldsymbol{\alpha}^{n+1}$ and κ^{n+1} $\Rightarrow$ Compute: $\mathbf{p}^{n+1}$ $\Rightarrow$ Store: $\boldsymbol{\sigma}^{n+1}$ $\Rightarrow$ Return to PDE solver
	If(False) $\Rightarrow$ Update: $\boldsymbol{\sigma}^{n+1}$ $\Rightarrow$ Return to PDE solver

Table 3.2

Direct Integration Algorithm for Multiphase EMMI Model at $\theta^0 < M_{start}$

Step 0: Compute Material Parameters

Step 1: At Time t = 0 (n=0), Material Initialization Procedure For i = 1,2 Phases

$\Rightarrow$ Assuming: $\theta^0 < M_{start}$, Therefore: $\boldsymbol{\sigma}^{1,(2)} = \mathbf{0}$
$\Rightarrow$ Evaluate Material Properties and Parameters for $i = 1$ at θ^0
$\Rightarrow$ Compute: $\boldsymbol{\sigma}^{1,(1)}$
$\Rightarrow$ Retrieve and Store State: $\boldsymbol{\alpha}^0$, κ^0, π and $\Delta\boldsymbol{\epsilon}_p^0$

Step 2: At Time t $>$ 0 (n$>$0), Material Integration Procedure

$\Rightarrow$ Update: θ^{n+1}
$\Rightarrow$ Evaluate Material Properties and Parameters For i = 1,2 Phases at θ^{n+1}
$\Rightarrow$ Compute: ϕ^{n+1} or π^{n+1}
$\Rightarrow$ Retrieve: $\boldsymbol{\sigma}^n$, $\boldsymbol{\alpha}^n$, κ^n and $\Delta\boldsymbol{\epsilon}_p^n$
$\Rightarrow$ Compute: $\boldsymbol{\sigma}^{(i),n+1}$ For i = 1,2 Phases
$\Rightarrow$ Decompose: $\boldsymbol{\sigma}^{(i),n+1}$ into $\mathbf{s}^{(i),n+1}$ and $\mathbf{p}^{(i),n+1}$
$\Rightarrow$ Determine Magnitude of Plastic Deformation: For i = 1,2 Phases
$\Rightarrow$ Evaluate: $\sqrt{\frac{3}{2}}\ \mathbf{s}^{(i),n+1} - \frac{2}{3}\boldsymbol{\alpha}^{(i),n}\ \pm \pi > \left(\kappa^{(i),n} + Y^{(i)}\right)$

If(True)
$\Rightarrow$ Evaluate: $\Delta\boldsymbol{\epsilon}_p^{(i)}$ or $\Delta\mathbf{d}_p^{(i)}$
$\Rightarrow$ Compute: $\boldsymbol{\alpha}^{(i),n+1}$ and $\kappa^{(i),n+1}$
$\Rightarrow$ Compute: $\mathbf{p}^{(i),n+1}$
$\Rightarrow$ Store: $\boldsymbol{\sigma}^{(i),n+1}$ For i = 1,2 Phases
$\Rightarrow$ Return to PDE solver

If(False)
$\Rightarrow$ Update: $\boldsymbol{\sigma}^{(i),n+1}$, ϕ^{n+1} and π^{n+1}
$\Rightarrow$ Return to PDE solver

Figure 3.5 shows the a fit of EMMI state variable model to experimental data for 5120 steel.

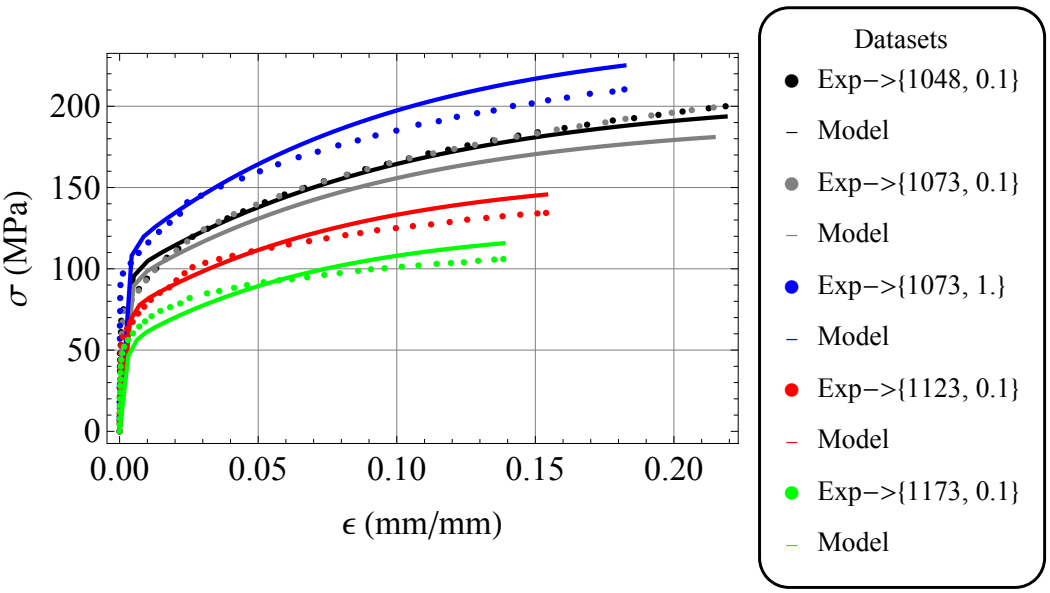

Figure 3.4

EMMI model for 5120 austenite steel at uniaxial tension.

In other to get a qualitative feel for how the local thermal histories affect phase transformation, three multiphase EMMI material point simulation (mmps) runs were performed at 100C/s, 200C/s and 300C/s cooling rates. The transformation kinetics Figure 3.6 shows a rapid transformation from austenite to martensite at higher cooling rates. The deviatoric stress in the austenite Figure 3.7 and martensite Figure 3.8 phases increases as the transformation proceeds. Though these runs only indicate the effect of cooling rate at a point they help qualitatively determine how the the deformation at juxtaposed material points would interact to cause deformation due to gradients in temperature.

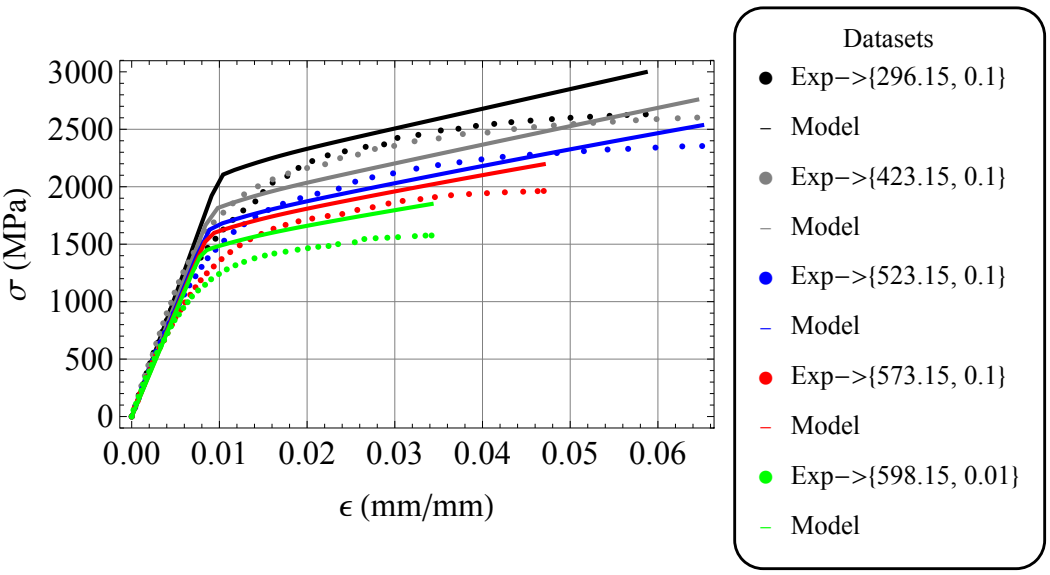

Figure 3.5

EMMI model for 5120 martensite steel at uniaxial tension.

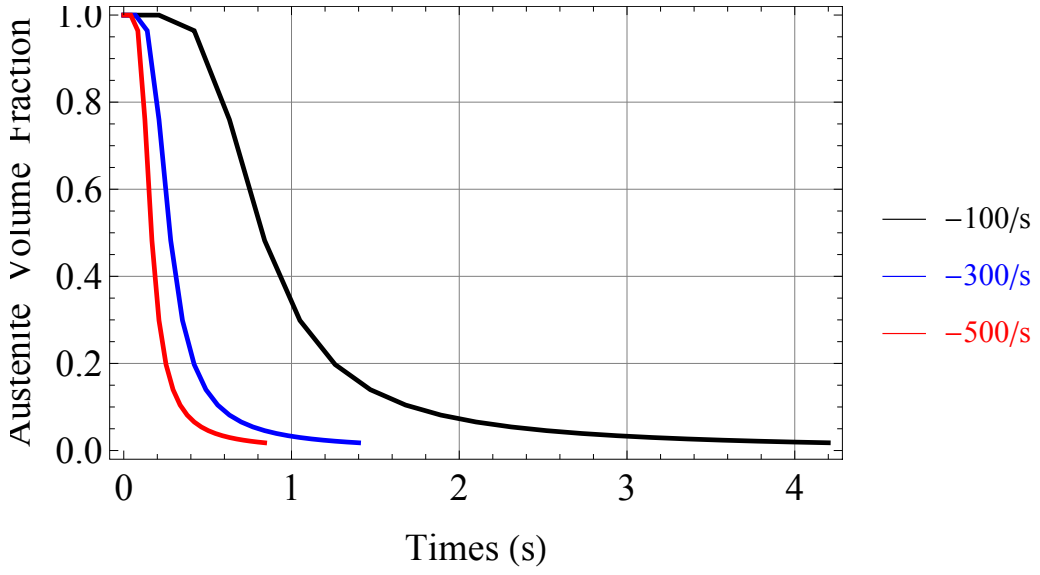

Figure 3.6

Multiphase EMMI model with Lusk model at 100C/s, 200C/s and 300C/s and 0.2%C.

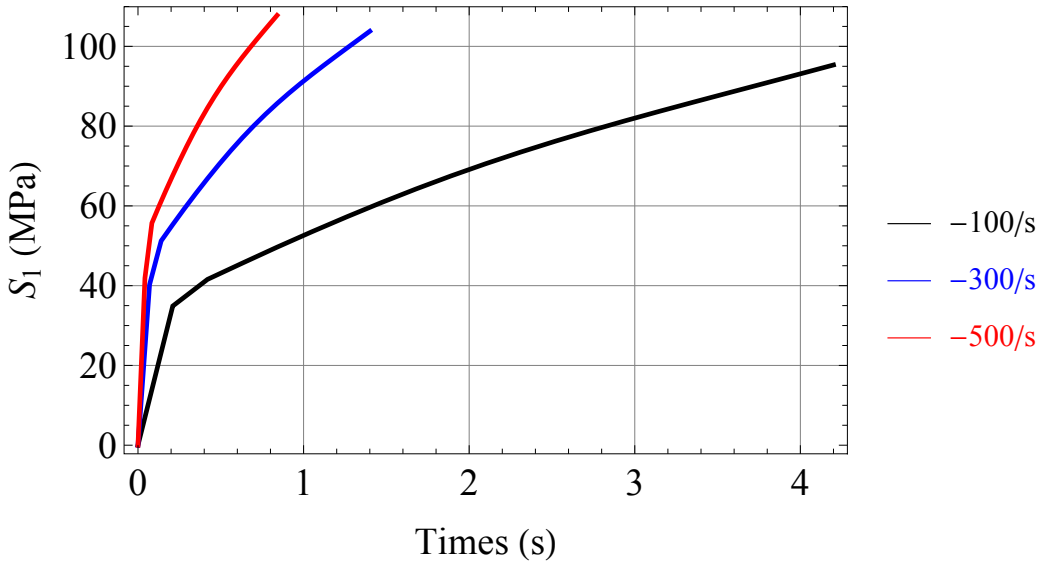

Figure 3.7

Multiphase EMMI model with Lusk model showing $\acute{\sigma}$ for austenite at 100C/s, 200C/s and 300C/s and 0.2%C.

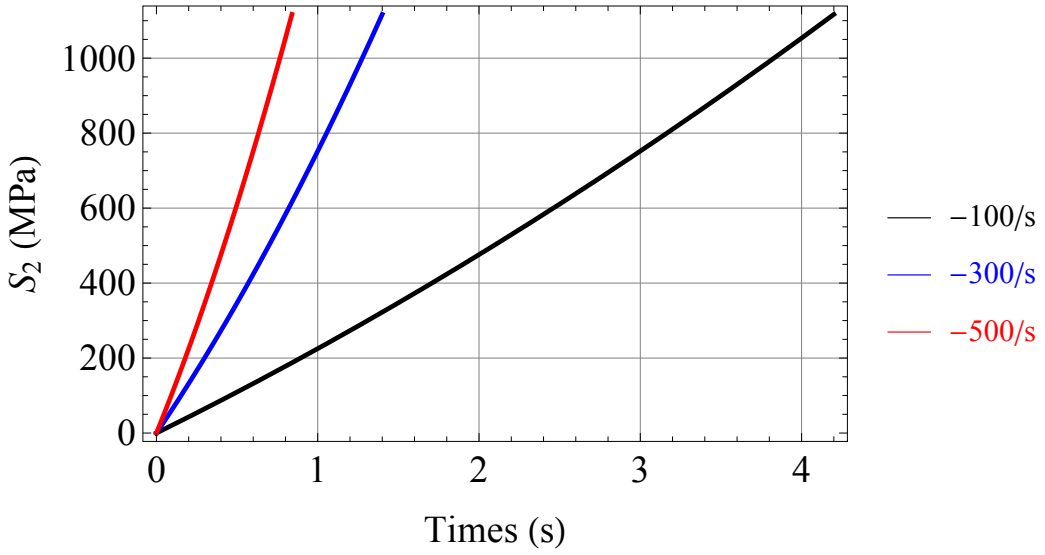

Figure 3.8

Multiphase EMMI with Lusk model showing $\acute{\sigma}$ for martensite at 100C/s, 200C/s and 300C/s and 0.2%C.

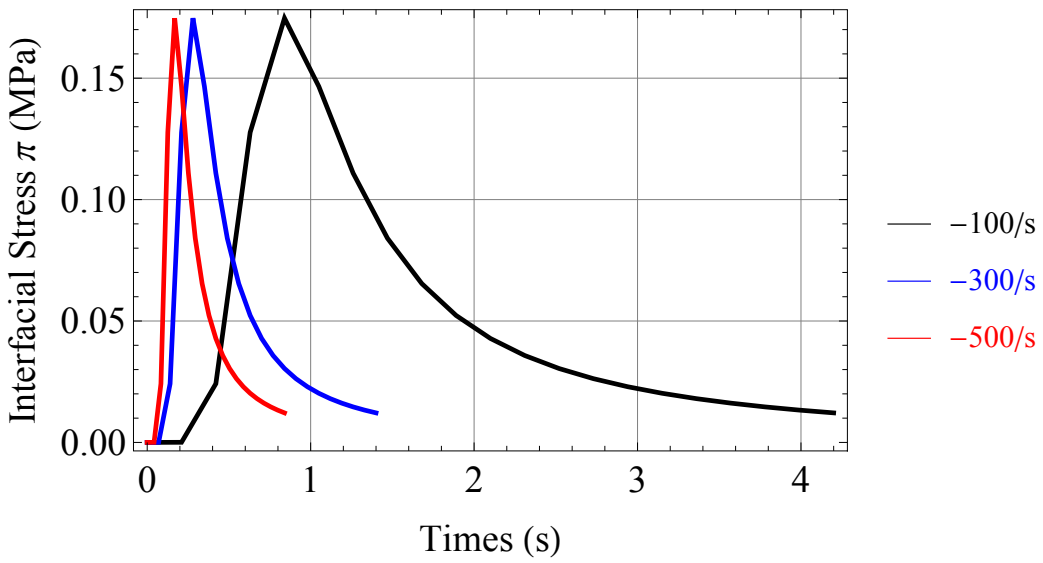

Figure 3.9

Interfacial for multiphase EMMI model with Lusk model at 100C/s, 200C/s and 300C/s and 0.2%C.

The carbon content effect on the mechanical response was investigated Figure 3.10, Figure 3.11 and Figure 3.12. The transformation kinetics coupled with the multiphase EMMI model for a fixed cooling rate of 100/s at a carbon content ranging from 0.05% to 0.2%. Prantil et al. [87] determined that the rate of transformation was faster as the carbon content was increased. The results here show a similar qualitative behavior when coupled with the EMMI mechanical response. The field variables however show no change in the mechanical response.

Figure 3.13 shows the additional straining induced by the transformation accounted for by the interfacial stress acting as a forward stress in the austenite and a backward stress in the martensite. The percentage of carbon content controls the smoothness of the rate of additional deformation due to transformation from austenite to martensite. Though

these simulation only indicate the effect of carbon content at a point they help qualitatively determine how carbon gradients at juxtaposed material points affect the transformation kinetics.

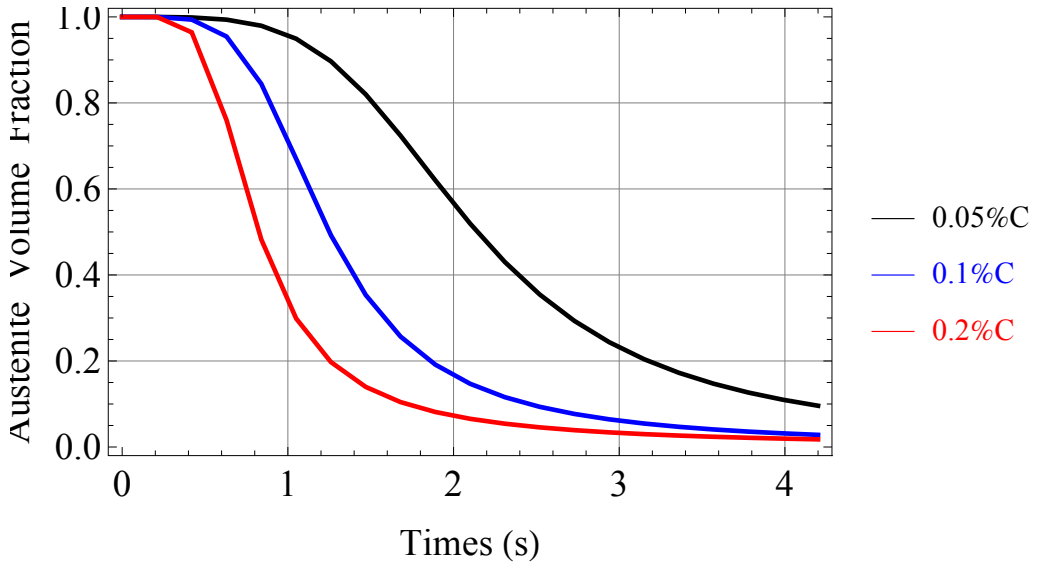

Figure 3.10

Multiphase EMMI with Lusk kinetics showing $1-\phi$ at 100C/s for %C = 0.05, 0.1 and 0.2.

3.5 Summary

We premised this investigation with a consistent thermodynamic framework and extended the single phase Evolving Microstructural Model of Inelasticity (EMMI) internal state variable model to multiphase affirming that the interaction between coexisting phases is through an interfacial stress. Following this, we employed a self-consistent polycrystalline model in order to partition each individual phase's strain field ensuring a hybrid

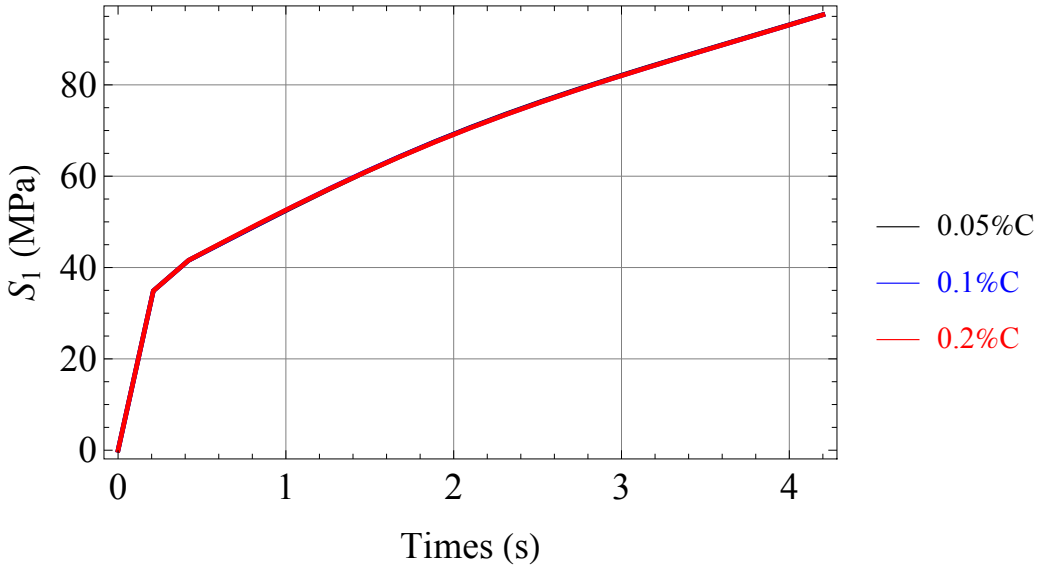

Figure 3.11

Multiphase EMMI with Lusk model showing $\acute{\sigma}$ for austenite at 100C/s and %C = 0.05, 0.1 and 0.2

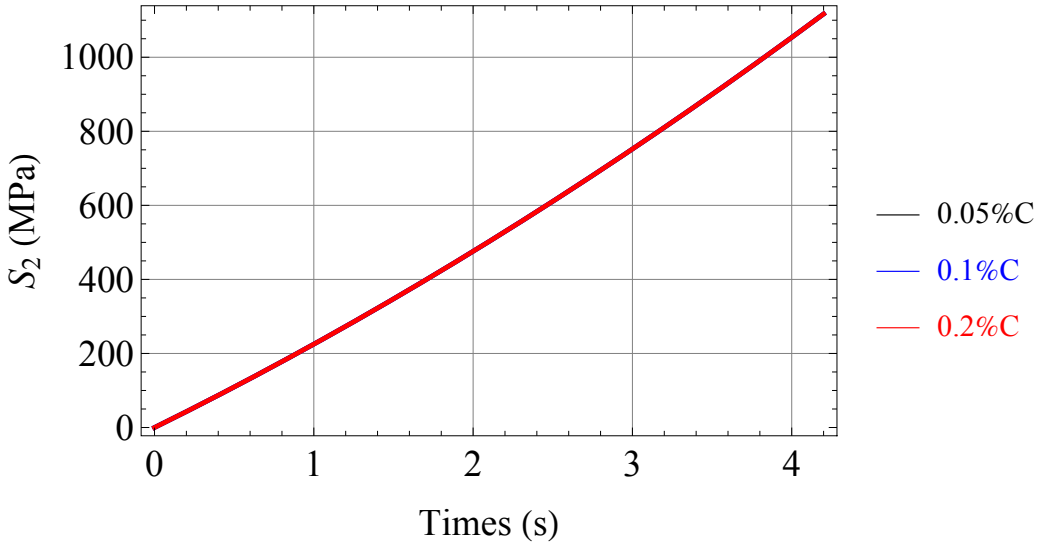

Figure 3.12

Multiphase EMMI with Lusk model showing $\acute{\sigma}$ for martensite at 100C/s and %C = 0.05, 0.1 and 0.2.

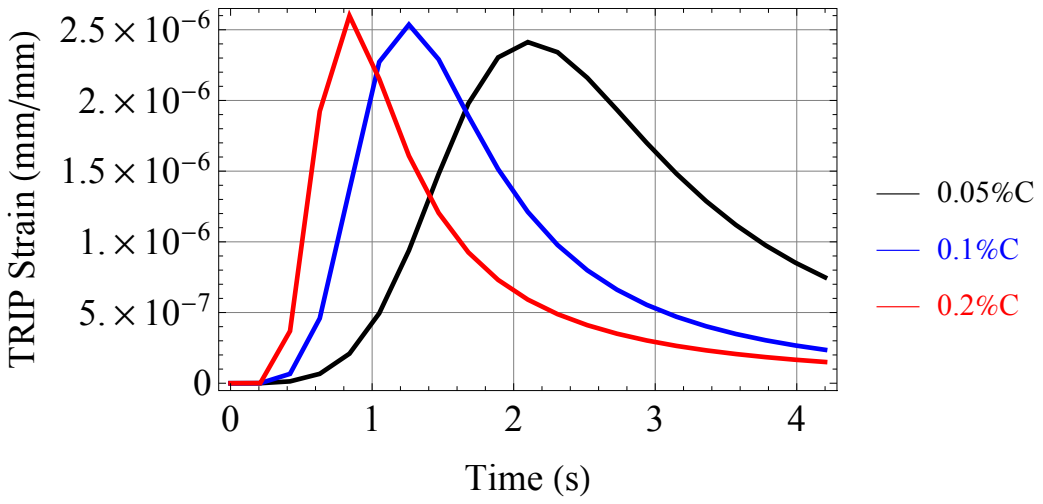

Figure 3.13

Multiphase EMMI with Lusk model showing TRIP strain at 100C/s for %C = 0.05, 0.1 and 0.2.

between compatibility and equilibrium. With a synthesis of the aforementioned ideas, the additional transformation plasticity (TRIP) is numerically accounted for by modifying each phase's flowrule to accommodate an interfacial stress. Further, we coupled the mechanical multiphase model equations with the previously developed non-diffusional phase transformation kinetics model developed by Lusk [51, 72, 73].

As noted by Ferguson et al. [33], necessary material processing routines not limited to quenching, welding or heat treatment produce high thermal gradients that lead to a fast transformation rates, most of which are experimentally challenging to capture. With this mind, it is conceivable that a well premised mathematical and physical model would serve as a useful numerical tool in the material fabrication industry.

CHAPTER 4

SUMMARY

4.1 Summary

Heat treatment for the purpose of material strengthening is accompanied by residual stresses and distortion. During these processing steps, steel alloys experience a phase change that in turn modify their overall mechanical response. To properly account for the cumulative composite behavior, the mechanical response, transformation kinetics and subsequent interaction of each phase have to be properly accounted for.

With aforementioned statements, the goal of this investigation was to develop a multiphase model capable of predicting and therefore aiding in controlling dimensional changes, distortion and residual stress in parts. Such a model must have several features. Foremost,it must be premised on a consistent thermodynamic framework. In addition, it must have the ability to predict the mechanical response of individual phases. Lastly, the model must capture the transformation kinetics of individual phases while physically incorporating their effects on the mechanical model.

To achieve the aforementioned objectives, a consistent thermodynamic framework was developed. Following this, the single phase EMMI internal state variable model was extended to multiphase affirming that the interaction between coexisting phases is through an interfacial stress. Since the efficacy of a multiphase model is dependent on its ability to

capture the behavior of constituents phases and their subsequent interaction, a physically based self-consistent partitioning algorithm was introduced. With a combination of the above, TRIP was numerically accounted for by modifying each phase's flowrule to accommodate an interfacial stress. In addition, for simulating the cohabitation of two phases, the mechanical multiphase model equations are coupled with a previously developed non-diffusional phase transformation kinetic model proposed by Lusk [51, 72, 73].

Here a two-phase system was implemented and qualitatively associated with austenite and martensite. Available was experimental data of 5120 steel over a limited strain rate and temperature regime. The goal to eventually extend this work to all five phases in an attempt to modify and extend the approach taken previously by Bammann et al. [12–14, 16]. Of interest here are materials that undergo phase transformation that consequentially modifies their material macroscopic response. The belief is that a proper continuum mechanics based formulation with internal state variables is sufficient to capture the underlying physical phenomena.

A quantitative assessment of the material response and plastic flow based on the Taylor, Sachs and self-consistent approximation was carried out. Following this, a quantitative assessment of the multiphase EMMI material model coupled with the non-diffusive phase transformation kinetic model was carried out. Parameter identification for the mechanical response of both the austenite and martensite phases was performed using a gradient based optimization routine following previous works of Marin et al. [80]. Parameters used here for the transformation kinetics are published values based on previous works of Lusk et

al. [51,72,73]. For the sake of simplicity material hardening dependence on carbon content was not accounted for.

REFERENCES

[1] F. Abrassart, "Influence des transformations martensitiques sur les propriétés mécaniques des alliages du système Fe-Ni-Cr-C," *PhD Report, Université de Nancy, France*, 1972.

[2] K. W. Andrew, ," *JIST*, vol. 203, 1965, pp. 721–727.

[3] I. Arthur D. Little, *Prediction and Control of Heat Treat Distortion of Helicopter Gears*, Interim Report to the U. S Army No. 41686, 1993.

[4] M. Ashby, "The deformation of plastically non-homogeneous materials," *Philosophical Magazine*, vol. 21, no. 170, 1970, pp. 399–424.

[5] M. Avrami, "Kinetics of Phase Change. I General Theory," *The Journal of Chemical Physics*, vol. 7, no. 12, 1939, pp. 1103–1112.

[6] M. Avrami, "Kinetics of Phase Change. II Transformation-Time Relations for Random Distribution of Nuclei," *The Journal of Chemical Physics*, vol. 8, no. 2, 1940, pp. 212–224.

[7] M. Avrami, "Granulation, Phase Change, and Microstructure Kinetics of Phase Change III," *The Journal of Chemical Physics*, vol. 9, no. 2, feb 1941, pp. 177–184.

[8] E. Bain, "The Nature of Solid Solutions," *Chem. Metall. Eng*, vol. 28, 1923, pp. 21–24.

[9] J. Ball, "Existence of solutions in finite elasticity," *Proceedings of the IUTAM Symposium on Finite Elasticity*. Springer, 1982, pp. 1–12.

[10] D. Bammann, M. Chiesa, and G. Johnson, "Modeling large deformation and failure in manufacturing processes," *Theoretical and Applied Mechanics*, 1996, pp. 359–376.

[11] D. Bammann, M. Chiesa, and G. Johnson, "Modeling large deformation and failure in manufacturing processes," *Theoretical and Applied Mechanics 1996: Proceedings of the XIXth International Congress of Theoretical and Applied Mechanics, Kyoto, Japan, 25-31 August 1996*. North Holland, 1997, vol. 19, p. 359.

[12] D. Bammann, V. Prantil, and A. Kumar, *Development of a carburizing and quenching simulation tool: a material model for low carbon steels undergoing phase transformations*, Tech. Rep., Lawrence Livermore National Lab., CA (United States), 1996.

[13] D. Bammann, V. Prantil, A. Kumar, J. Lanthrop, D. Mosher, M. Lusk, H.-J. Jou, G. Krauss, and W. Elliott, *A material model for low carbon steels undergoing phase transformations*, In: Totten G, Proceedings of the Second International Conference on Quenching and the Control of Distortion. Warrendale, PA, 1996.

[14] D. Bammann, V. Prantil, and J. Lathrop, "A Model of Phase Transformation Plasticity," *Modelling of Casting, Welding and Advanced Solidification Processes VII*, 1995, pp. 275–285.

[15] D. J. Bammann, "Modeling temperature and strain rate dependent large deformations of metals," *Applied Mechanics Reviews*, vol. 43, 1990, p. 312.

[16] D. J. Bammann, V. C. Prantil, and J. F. Lathrop, "A plasticity model for materials undergoing phase transformations," *Simulation of Materials Processing: Theory, Methods and Applications. NUMIFORM*, vol. 95., 1995, p. 219 224.

[17] D. J. . M. Bammann, D. A. . Hughes, D. A. . Moody, N. R. . Dawson, and Paul, *Using spatial gradients to model localization phenomena*, Sandia Report SAND99-8588, Sandia National Laboratories, Livermore, CA, 1999.

[18] Z. Bo and D. C. Lagoudas, "Thermomechanical modeling of polycrystalline SMAs under cyclic loading, Part I: theoretical derivations," *International Journal of Engineering Science*, vol. 37, no. 9, 1999, pp. 1089 – 1140.

[19] N. Böck and G. Holzapfel, "A Large Strain Continuum and Numerical Model for Transformation Induced Plasticity (TRIP)," *Fifth World Congress on Computational Mechanics, pages–, Austria*, 2002.

[20] S. Bodner, *Unified Plasticity for Engineering Applications*, Mathematical concepts and methods in science and engineering. Kluwer Academic, 2002.

[21] B. Budiansky and T. Te Wu, *Theoretical prediction of plastic strains of polycrystals*, Contract Nonr 1866(02) Technical report. Division of Engineering and Applied Physics, Harvard University, 1961.

[22] W. Callister and D. Rethwisch, *Materials Science and Engineering: An Introduction, Eigth Edition Binder Ready Version*, John Wiley & Sons, 2010.

[23] B. D. Coleman and M. E. Gurtin, "Thermodynamics with Internal State Variables," *The Journal of Chemical Physics*, vol. 47, 1967, p. 597.

[24] B. D. Coleman and V. J. Mizel, "Existence of caloric equations of state in thermodynamics," *The Journal of Chemical Physics*, vol. 40, 1964, p. 1116.

[25] B. D. Coleman and W. Noll, "The thermodynamics of elastic materials with heat conduction and viscosity," *Archive for Rational Mechanics and Analysis*, vol. 13, no. 1, 1963, pp. 167–178.

[26] A. Comsol, "COMSOL multiphysics users guide," *Version: September*, 2005.

[27] D. Dubois, J. Devaux, and J. B. Leblond, "Numerical Simulation of a Welding Operation: Calculation of Residual Stresses and Hydrogen Diffusion," *Proceedings of the Fifth International Conference on Pressure Vessel Technology*, vol. 2, 1984, pp. 1210–1239.

[28] J. Ericksen, "Equilibrium of bars," *Journal of Elasticity*, vol. 5, 1975, pp. 191–201.

[29] J. D. Eshelby, "The Determination of the Elastic Field of an Ellipsoidal Inclusion, and Related Problems," *Proceedings of the Royal Society A Mathematical Physical and Engineering Sciences*, vol. 241, no. 1226, 1957, pp. 376–396.

[30] J. D. Eshelby, "The Elastic Field Outside an Ellipsoidal Inclusion," *Proceedings of the Royal Society of London Series A Mathematical and Physical Sciences*, vol. 252, no. 1271, 1959, pp. 561–569.

[31] Y. Estrin and H. Mecking, "A unified phenomenological description of work hardening and creep based on one-parameter models," *Acta Metallurgica*, vol. 32, no. 1, 1984, pp. 57–70.

[32] B. L. Ferguson, A. M. Freborg, G. Petrus, and M. L. Callabresi, "Predicting the heat-treat response of a carburized helical gear.," *Gear Technology*, vol. 19, no. 6, 2002, pp. 20–25.

[33] B. L. Ferguson, Z. Li, and A. Freborg, "Modeling heat treatment of steel parts," *Computational Materials Science*, vol. 34, no. 3, 2005, pp. 274–281.

[34] C. O. Frederick and P. Armstrong, "A mathematical representation of the multiaxial Bauschinger effect," *Materials at High Temperatures*, vol. 24, no. 1, 2007, pp. 1–26.

[35] H. J. Frost and M. F. Ashby, "Deformation mechanism maps: the plasticity and creep of metals and ceramics," 1982.

[36] D. Gigou, *Plasticité de transformation: Cas de la transformation martensitique*, 1985.

[37] J. Giusti, *Contraintes et déformations résiduelles d'origine thermique: application au soudage et à la trempe des aciers*, doctoral dissertation, 1981.

[38] J. A. Goldak, *Modeling Thermal Stresses and Distortions in Welds*, Recent Trends in Welding Science and Technology,ASM International, S. A. David and M. Vitek, (Gatlinburg, TN, 1990.

[39] J. A. Goldak et al., *Computational Weld Mechanics*, Proceedings of the International Symposium on Computer Modeling of Fabrication Processes and Constitutive Behavior of Metals, (Ottawa, Canada 1986), 1986.

[40] J. A. Goldak et al., *Coupling Heat Transfer, Microstructure Evolution and Thermal Stress Analysis in Weld Mechanics*, Proceedings of the IUTAM Symposium, (Lulea, Sweden 1991), 1991.

[41] G. W. Greenwood and R. H. Johnson, "The Deformation of Metals Under Small Stresses During Phase Transformations," *Proceedings of The Royal Society of London. Series A, Mathematical and Physical Sciences (1934-1990)*, vol. 283, 1965, pp. 403–422.

[42] M. E. Gurtin, "Generalized Ginzburg-Landau and Cahn-Hilliard equations based on a microforce balance," *Physica D: Nonlinear Phenomena*, vol. 92, no. 3, 1996, pp. 178–192.

[43] H. Hallberg, P. Hkansson, and M. Ristinmaa, "A constitutive model for the formation of martensite in austenitic steels under large strain plasticity," *International Journal of Plasticity*, vol. 23, no. 7, 2007, pp. 1213 – 1239.

[44] R. Hill, "The essential structure of constitutive laws for metal composites and polycrystals," *Journal of the Mechanics and Physics of Solids*, vol. 15, no. 2, 1967, pp. 79–95.

[45] D. A. . B. Hughes, D. J. . Godfrey, W. . P. Andrew, V. C. . Holm, and Elizabeth, *Capturing recrystallization of metals with a multi-scale materials model*, Sandia Report SAND2000-8232, Sandia National Laboratories, Livermore, CA, Apr. 2000.

[46] T. Inoue and K. Arimoto, "Development and implementation of cae system hearts for heat treatment simulation based on metallo-thermo-mechanics," *Journal of Materials Engineering and Performance*, vol. 6, no. 1, 1997, pp. 51–60.

[47] T. Inoue, D.-Y. Ju, and K. Arimoto, "Metallo-Thermo-Mechanical Simulation of Quenching Process–Theory and Implementation of Computer Code" Hearts"," *Quenching and Distortion Control*, 1992, pp. 205–212.

[48] S. R. Institute and Farmatome, *SYSWELD-A Predictive Model for Heat Treat Distortion*, Presentation at the National Centerfor Manufacturing Sciences, Ann Arbor, Michigan, April 14, 1992.

[49] C. . international conference on quenching and O. U. S. the control of distortion, Cleveland, eds., *Development of a carburizing and quenching simulation tool: A material model for low carbon steels undergoing phase transformations*, 1996.

[50] W. A. Johnson and R. F. Mehl, "Reaction kinetics in processes of nucleation and growth," *Trans. Aime*, vol. 135, no. 8, 1939, pp. 396–415.

[51] H.-J. Jou and M. T. Lusk, "Comparison of Johnson-Mehl-Avrami-Kologoromov kinetics with a phase-field model for microstructural evolution driven by substructure energy," *Physical Review B*, vol. 55, no. 13, 1997, p. 8114.

[52] A. Khan and S. Huang, *Continuum Theory of Plasticity*, Wiley-Interscience publication. Wiley, 1995.

[53] U. Kocks and H. Mecking, "A mechanism for static and dynamic recovery," *Strength of metals and alloys*, 1980, pp. 345–350.

[54] U. Kocks, C. Tomé, H. Wenk, and H. Mecking, *Texture and Anisotropy: Preferred Orientations in Polycrystals and their Effect on Materials Properties*, Cambridge University Press, 2000.

[55] D. Koistine, "A general equation prescribing the extent of the austenite-martensite transformation in pure iron-carbon alloys and plain carbon steels," *acta metallurgica*, vol. 7, 1959, pp. 59–60.

[56] D. Koistinen and R. Marburger, "A simplified procedure for calculating peak position in X-ray residual stress measurements on hardened steel," *Trans. ASM*, vol. 51, 1959, p. 537.

[57] A. Kolmogorov, "On the Statistical Theory of Metal Crystallization," *Izv. Akad. Nauk SSSR, Ser. Math*, vol. 1, 1937, pp. 335–360, Computes density of fairly general Johnson-Mehl crystals and the probability that a point is not in a crystal yet.

[58] R. Krieg, J. Swearengen, and W. Jones, "A physically based internal variable model for rate dependent plasticity," *Unified Constitutive Equations for Creep and Plasticity*, Springer, 1987, pp. 245–271.

[59] E. Kroner, *Allgemeine kontinuumstheorie der versetzungen*, Arch, 1960.

[60] J. Leblond, *Simulation Num é America Welding - Mod é LITY Math é matic transformations M é tallurgiques - State Works Progress*, Tech. Rep., Technical Report TM / C DC/80.066, Framatome, 1980.

[61] J. Leblond, G. Mottet, and J. Devaux, "A theoretical and numerical approach to the plastic behaviour of steels during phase transformationsII. Study of classical plasticity for ideal-plastic phases," *Journal of the Mechanics and Physics of Solids*, vol. 34, no. 4, 1986, pp. 411–432.

[62] J. B. Leblond, J. Devaux, and J. C. Devaux, "Mathematical Modeling of Transformation Plasticity in Steels I: Case of Ideal-Plastic Phases," *International Journal of Plasticity*, vol. 5, 1989, pp. 551–572.

[63] J. B. Leblond, J. Devaux, and J. C. Devaux, "Mathematical Modeling of Transformation Plasticity in Steels II: Coupling With Strain Hardening Phenomena," *International Journal of Plasticity*, vol. 5, 1989, pp. 573–591.

[64] J.-B. Leblond, G. Mottet, and J. Devaux, "A theoretical and numerical approach to the plastic behaviour of steels during phase transformations - I. Derivation of general relations," *Journal of the Mechanics and Physics of Solids*, vol. 34, no. 4, 1986, pp. 395–409.

[65] J. B. Leblond, G. Mottet, and J. C. Devaux, "A Theoretical and Numerical Approach to the Plastic Behavior of Steels During Phase Transformations - II. Study of Classical Plasticity for Ideal-Plastic Phases," *J. Mech. Phys. Solids*, vol. 34, no. 4, 1986, pp. 411–432.

[66] E. H. Lee and D. T. Liu, "Finite strain plasticity particularly for plane waves," *Journal of Applied Physics*, vol. 38, 1967.

[67] V. I. Levitas, "Thermomechanical theory of martensitic phase transformations in inelastic materials," *International Journal of Solids and Structures*, vol. 35, no. 910, 1998, pp. 889 – 940.

[68] V. I. Levitas and D. L. Preston, "Three-dimensional Landau theory for multivariant stress-induced martensitic phase transformations .I. Austenite to martensite," *Phys. Rev. B*, vol. 66, Oct 2002, p. 134206.

[69] V. I. Levitas and D. L. Preston, "Three-dimensional Landau theory for multivariant stress-induced martensitic phase transformations. II. Multivariant phase transformations and stress space analysis," *Physical Review B*, vol. 66, no. 13, 2002, p. 134207.

[70] Z. Li, A. Freborg, B. Hansen, and T. Srivatsan, "Modeling the Effect of Carburization and Quenching on the Development of Residual Stresses and Bending Fatigue Resistance of Steel Gears," *Journal of Materials Engineering and Performance*, vol. 22, no. 3, 2013, pp. 664–672.

[71] Z.-c. Li and B. Ferguson, "Computer modeling and validations of steel gear heat treatment processes using commercial software DANTE," *Journal of Shanghai Jiaotong University (Science)*, vol. 16, no. 2, 2011, pp. 152–156.

[72] M. Lusk and H.-J. Jou, "On the rule of additivity in phase transformation kinetics," *Metallurgical and Materials Transactions A*, vol. 28, no. 2, 1997, pp. 287–291.

[73] M. Lusk, G. Krauss, and H.-J. Jou, "A balance principle approach for modeling phase transformation kinetics," *Le Journal de Physique IV*, vol. 5, no. C8, 1995, pp. C8–279.

[74] M. T. Lusk and Y.-K. Lee, "A global material model for simulating the transformation kinetics of low alloy steels," *7 th International Seminar of IFHT(International Federation for Heat Treatment and Surface Engineering)*, 1999, pp. 273–282.

[75] C. Magee and H. Paxton, *Transformation Kinetics, Microplasticity and Aging of Martensite in Fe-31Ni*, Carnegie Inst. of Technology, 1966.

[76] C. L. Magee, *Transformation Kinetics,Microplasticity and Aging of Martensite in Fe-31 Ni*, Carnegie Institute of Technology, 1966.

[77] J. Mandel, "Contribution théorique à l'étude de l'écrouissage et des lois de l'écoulement plastique," *Proc. 11th Int. Congr. Appl. Mech*, 1964, pp. 502–509.

[78] A. S. U. Manual, "version 5.7, 1997. Hibbitt, Karlsson and Sorensen," *Inc., Providence, Rhode Island*.

[79] S. U. Manual, "version SP3. 1," *Dassault Systemes, Sureness, France*, 2005.

[80] E. B. Marin, D. J. Bammann, R. A. Regueiro, and G. C. Johnson, *On the Formulation, Parameter Identification and Numerical Integration of the EMMI Model: Plasticity and Isotropic Damage*, SAN D2006-0200, Sandia National Laboratories, 2006.

[81] A. Miller, *Unified Constitutive Equations for Creep and Plasticity*, World Publishing Corporation, 1987.

[82] W. Mitter, *Umwandlungsplastizit "a t and Ber ü cksichtigung in the calculation of residual stresses*, Borntraeger-Verlag, 1987.

[83] J. N. and S. S., *Current Status of TRAST: A Material Model Subroutine System forthe Calculation of Quench Stressesin Steel,ABAQUS Users Conference Proceedings*, 1993.

[84] K. Naumenko and H. Altenbach, *Modeling of Creep for Structural Analysis*, Foundations of Engineering Mechanics. Springer-Verlag Berlin Heidelberg, 2007.

[85] E. Nes, "Recovery revisited," *Acta Metallurgica et Materialia*, vol. 43, no. 6, 1995, pp. 2189 – 2207.

[86] A. S. Oddy, J. A. Goldak, and J. M. J. McDill, "Transformation Plasticity and Residual Stresses in Single-Pass Repair Welds," *ASME Journal of Pressure Vessel Technology*, vol. 114, 1992, pp. 33–38.

[87] V. C. Prantil, M. L. Callabresi, J. F. Lathrop, G. S. Ramaswamy, and M. T. Lusk, "Simulating Distortion and Residual stresses in Caburized Thin Strips," *Journal of Engineering Materials and Technology*, vol. 125, 2003, pp. 116–124.

[88] G. Sachs, "Zur Ableitung einer Fliebedingung," *Mitteilungen der deutschen Materialprfungsanstalten*, Springer Berlin Heidelberg, 1929, pp. 94–97.

[89] S. Sjostrom, *The Calculation of Quench Stresses in Steel*, doctoral dissertation, Linkoping Univeristy, Sweden, 1982.

[90] S. Sjostrom, "Interactions and Constitutive Models for Calculating Quench Stresses in Steel," *Materials Science and Technology*, vol. 1, 1985, pp. 823–829.

[91] R. Stringfellow, D. Parks, and G. Olson, "A constitutive model for transformation plasticity accompanying strain-induced martensitic transformations in metastable austenitic steels," *Acta Metallurgica et Materialia*, vol. 40, no. 7, 1992, pp. 1703–1716.

[92] K. Tanaka and S. Nagaki, "A thermomechanical description of materials with internal variables in the process of phase transitions," *Ingenieur-Archiv*, vol. 51, no. 5, 1982, pp. 287–299.

[93] G. Taylor, "Analysis of plastic strain in a cubic crystal," *Stephen Timoshenko 60th Anniversary Volume*, 1938, pp. 218–224.

[94] G. Taylor and U. Dehlinger, "Strains in Crystalline Aggregate," *Deformation and Flow of Solids / Verformung und Fliessen des Festkrpers*, R. Grammel, ed., International Union of Theoretical and Applied Mechanics / Internationale Union fr Theoretische und Angewandte Mechanik, Springer Berlin Heidelberg, 1956, pp. 3–12.

[95] G. I. Taylor, *Plastic strain in metals*, 1938.

[96] D. Tjahjanto, S. Turteltaub, and A. Suiker, "Crystallographically based model for transformation-induced plasticity in multiphase carbon steels," *Continuum Mechanics and Thermodynamics*, vol. 19, no. 7, 2008, pp. 399–422.

[97] C. Truesdell and W. Noll, *The Non-Linear Field Theories of Mechanics*, Springer-Verlag, 1992.

[98] C. Truesdell and W. Noll, *The non-linear field theories of mechanics*, Springer, 2004.

[99] V. S. Warke, *Predicting the Response of Powder Metallurgy Steel Components to Heat Treatment*, doctoral dissertation, Worcester Polytechnic Institute, 2008.

[100] G. Webster, "A widely applicable dislocation model of creep," *Philosophical Magazine*, vol. 14, no. 130, 1966, pp. 775–783.

[101] M. S. Wechsler, *On the Theory of the Formation of Martensite.*, 1954.

[102] S. Zhang, Z. Li, and B. L. Ferguson, "Effect of Carburization on the Residual Stress and Fatigue Life of a Transmission Shaft," *Heat Treating: Proceedings of the 23rd Heat Treating Society Conference, September 25-28, 2005, David L. Lawrence Convention Center, Pittsburgh, Pennsylvania*. ASM International (OH), 2006.

APPENDIX A

EXPERIMENTAL AND NUMERICAL DATA FOR AUSTENITE

Experimental and numerical data for austenite:

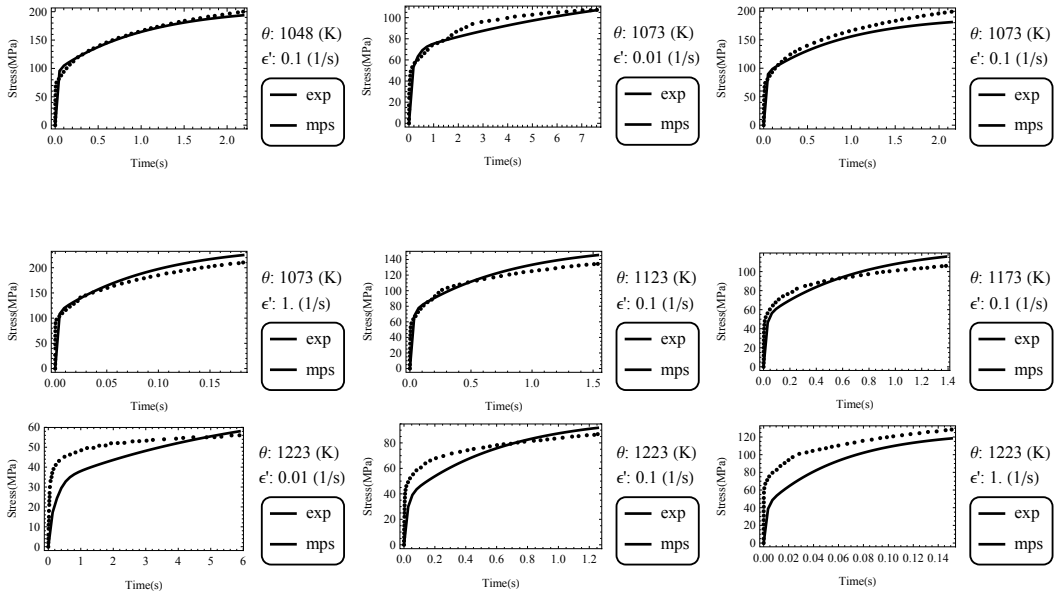

Figure A.1

EMMI model response to uniaxial tension data for 5120 austenite steel at various strain rates and temperatures

APPENDIX B

EXPERIMENTAL AND NUMERICAL DATA FOR MARTENSITE

Experimental and numerical data for martensite:

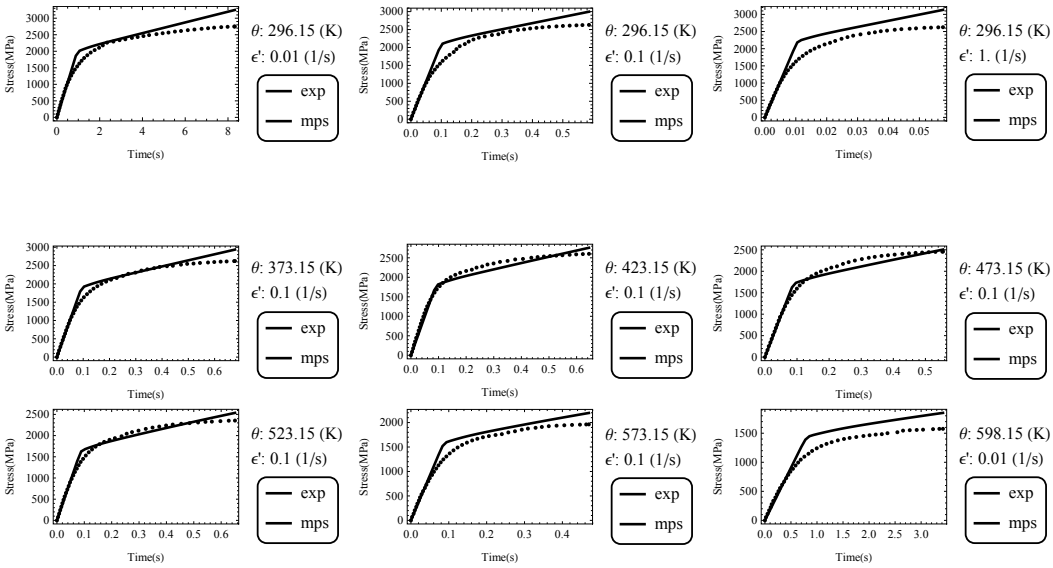

Figure B.1

EMMI model response to uniaxial tension data for 5120 martensite steel at various strain rates and temperatures

APPENDIX C

FORMS OF MATERIAL PARAMETERS

C.1 Form of EMMI Model Parameter

Effective Plastic Flow Parameters:

$$n(\theta) = \frac{c(9)}{\theta} + c(1) \tag{C.1}$$

$$f(\theta) = c(2)Exp(\frac{-Q(1)}{\theta}) \tag{C.2}$$

Kinematic Hardening Parameters:

$$C_{\boldsymbol{\alpha}}(\theta) = c(11) \tag{C.3}$$

$$h(\theta) = c(4) \tag{C.4}$$

$$rd(\theta) = c(3)Exp(\frac{-Q(2)}{\theta}) \tag{C.5}$$

Isotropic Hardening Parameters:

$$C_{\kappa}(\theta) = c(12) \tag{C.6}$$

$$H(\theta) = c(6) \tag{C.7}$$

$$R_d(\theta) = c(5)Exp(\frac{-Q(3)}{\theta}) \tag{C.8}$$

$$R_s(\theta) = c(7)Exp(\frac{-Q(4)}{\theta}) \tag{C.9}$$

$$Q_s(\theta) = c(10)Exp(\frac{-Q(5)}{\theta}) \tag{C.10}$$